Copyright Warning & Restrictions

The copyright law of the United States (Title 17, United States Code) governs the making of photocopies or other reproductions of copyrighted material.

Under certain conditions specified in the law, libraries and archives are authorized to furnish a photocopy or other reproduction. One of these specified conditions is that the photocopy or reproduction is not to be "used for any purpose other than private study, scholarship, or research." If a, user makes a request for, or later uses, a photocopy or reproduction for purposes in excess of "fair use" that user may be liable for copyright infringement,

This institution reserves the right to refuse to accept a copying order if, in its judgment, fulfillment of the order would involve violation of copyright law.

Please Note: The author retains the copyright while the New Jersey Institute of Technology reserves the right to distribute this thesis or dissertation

Printing note: If you do not wish to print this page, then select "Pages from: first page # to: last page #" on the print dialog screen

ABSTRACT

FUEL-RICH COMBUSTION OF ETHYLENE AND AIR IN A TWO STAGE TURBULENT FLOW REACTOR

by
Tara Byrnes Salem

This thesis presents experimental and modeling results from the combustion of ethylene and air in a two stage turbulent flow reactor. This work is motivated by the continuing concern over combustion by-products. The first half of the research effort focused on the validation of the reactor as a perfectly stirred reactor and a plug flow reactor (PSR+PFR) sequence. Using four detailed reaction mechanisms, measured concentrations of carbon oxides, oxygen, and light hydrocarbon concentrations were modeled. Within the accuracy of the data, the mechanism of Mao (1995) yielded the best results. However, it was observed that the success of the reactor validation effort is dependent on the chosen mechanism. The second half of this work focused on the fuel-rich combustion of ethylene and air using an on-line microtrap to concentrate the combustion samples. Although the microtrap demonstrated potential, its applicability at high fuel equivalence ratios was hindered by excessive hydrocarbon concentrations. However, benzene, a known precursor to larger and more toxic combustion by-products, was identified and quantified with the microtrap. The benzene data were qualitatively modeled using a mechanism developed by Zhong (1996). Light hydrocarbons and stable combustion species measured in packed columns were accurately modeled with the Mao mechanism.

FUEL-RICH COMBUSTION OF ETHYLENE AND AIR IN A TWO STAGE TURBULENT FLOW REACTOR

by
Tara Byrnes Salem

A Thesis
Submitted to the Faculty of
New Jersey Institute of Technology
in Partial Fulfillment of the Requirements for the Degree of
Master of Science in Chemical Engineering

Department of Chemical Engineering,
Chemistry, and Environmental Science

October 1996

APPROVAL PAGE

FUEL-RICH COMBUSTION OF ETHYLENE AND AIR IN A TWO STAGE TURBULENT FLOW REACTOR

Dr. Robert Barat, Thesis Advisor — Date
Associate Professor of Chemical Engineering, NJIT

Dr. Dana Knox, Committee Member — Date
Associate Professor of Chemical Engineering, NJIT

Dr. Somenath Mitra, Committee Member — Date
Associate Professor of Chemistry, NJIT

BIOGRAPHICAL SKETCH

Author: Tara Byrnes Salem

Degree: Master of Science in Chemical Engineering

Date: October 1996

Undergraduate and Graduate Education:

- Master of Science in Chemical Engineering
  New Jersey Institute of Technology, Newark, NJ, 1996

- Bachelor of Science in Chemical Engineering
  Worcester Polytechnic Institute, Worcester, MA, 1994

Major: Chemical Engineering

Presentations:

Tara B. Salem, Fuhe Mao, and Robert B. Barat, "Effect of Steam Injection on the Simultaneous Air-Staged Incineration of Fuel-Bound Nitrogen and Fuel-Bound Chlorine." *The Eastern States Combustion Institute*, Worcester Polytechnic Institute - Worcester, MA, 1995.

Tara B. Salem, Robert B. Barat, and Charles Bass, "The Incineration of CH_2Cl_2 and CCl_4 in an Air-Staged Two Zone Turbulent Reactor." *The Eastern States Combustion Institute*, Worcester Polytechnic Institute - Worcester, MA, 1995.

ACKNOWLEDGMENT

I would like to send my deepest and most sincere appreciation to Dr. Robert Barat. Thanks to his support, enthusiasm, and friendship, my time at NJIT has been one of the most positive experiences of my life.

I also send my thanks to the members of my thesis committee, Dr. Dana Knox and Dr. Somenath Mitra.

During the past two years, I have been assisted by many terrific students and faculty at NJIT. In particular, I owe thanks to Clint Brockway, Ann Marie Flynn, Dr. Fuhe Mao, and Steven Wojdyla.

There are many other important people who I would like to thank. I owe everything to my family, especially my parents, Timothy and Michele, and my brother, Zachary. Mere words cannot express my appreciation for all they have done for me throughout the years. Also, I wish to thank one very special person who I have met and fallen in love with during my stay in New Jersey - thanks to my best friend, Michael Maguire. His tireless support has made this research effort a success. I could not have done it without him. There are many other friends that I would like to thank. One in particular is my dearest friend, Huifang Fan. Her good heart and sincere dedication to academics will serve as an inspiration to me always.

TABLE OF CONTENTS

TABLE OF CONTENTS
(Continued)

LIST OF TABLES

LIST OF FIGURES

LIST OF FIGURES
(Continued)

CHAPTER 1

INTRODUCTION

Although common combustion (incineration) emissions of concern are carbon monoxide (CO) and nitrogen oxides (NO/NO_2), this research focuses on products of incomplete combustion (PICs), such as benzene (C_6H_6) and acetylene (C_2H_2). PICs can often result from a lack of good mixing between the waste, fuel, and air. The poor mixing can lead to localized pockets of gas whose composition vary widely. When these pockets do not burn completely, products of incomplete combustion can form. These PICs, in turn, can become seeds for molecular weight growth and soot formation, thereby resulting in potentially more hazardous emissions than the original waste being eliminated.

A collaborative effort has been forged between combustion research groups at New Jersey Institute of Technology (NJIT) and Massachusetts Institute of Technology (MIT) in order to attain a better understanding of the formation and emission of PICs, which are due to the combined effects of turbulent mixing and chemical kinetics. The experimental tasks have been coordinated and divided between the two institutions in an effort to generate a cohesive and extensive data base. Each group is using ethylene (C_2H_4) as the fuel and methyl chloride (CH_3Cl) and methylene chloride (CH_2Cl_2) as the simulated hazardous wastes. Both NJIT and MIT utilize a well characterized, two-stage turbulent flow combustion facility, but the MIT reactor has been modified slightly to allow for radial dopant injections into the second zone. In order to see the effects of imperfect turbulent mixing, the MIT group runs their first stage under fuel-lean (i.e. excess air) conditions and then injects the dopant at the entrance of the second stage. The

second stage is considered non-premixed under these conditions. Even with the injection, overall fuel-lean conditions are maintained. Preliminary work (Sarofim et al. 1996) has shown that even under these fuel-starved conditions, some PICs such as benzene have been measured. Since the production of such PICs is only favored under very fuel-rich conditions, there must be localized pockets of fuel-rich gases present due to incomplete mixing.

While the MIT group focuses on the non-premixed fuel-lean work, the NJIT group is performing premixed fuel-rich tests, both with and without the chlorinated dopant. This will therefore provide the minimum fuel equivalence ratio (ϕ)* that must be achieved before PICs can be formed, both within the NJIT fuel-rich reactor and the fuel-rich pockets generated within the MIT fuel-lean reactor. The following thesis focuses on the desired chlorine-free, fuel-rich, premixed conditions. All remaining premixed chlorine runs at NJIT are work-in-progress and will be performed by other individuals.

* Fuel equivalence ratio is defined as the actual molar fuel to air ratio divided by the stoichiometric molar fuel to air ratio.

1.1 Objectives

The main goal of this research has been to establish a data set for premixed C_2H_4/air fuel-rich combustion as a baseline for later CH_2Cl_2-doped runs. The production of PICs and the resulting molecular weight growth have been investigated. The specific objectives of this thesis have been to:

1. Rebuild a two-stage reactor and validate the facility using known combustion reaction mechanisms.
2. Investigate the combustion of ethylene focusing on the production of PICs and higher molecular weight compounds.
3. Model these combustion processes using established elementary reaction mechanisms and compare with experimental data.

1.2 Research Approach

This study used a two-staged turbulent flow combustion chamber. Previous work (Mao 1995) using the same system validated the combustor as a perfectly stirred reactor (PSR) + plug flow reactor (PFR) sequence. This type of reactor has been used (Beer et al. 1983) to simulate many industrial furnaces and incinerators, especially those with gaseous or liquid feed nozzles and swirl-stabilized turbulent flame zones.

The ethylene experiments for this work were performed as follows. The reactor was first validated as a PSR + PFR sequence based on the stable species concentrations and subsequent model simulations. Additional runs were then performed to study the trace species. In order to enhance the production of both PICs and higher molecular weight compounds, the reactor was run at fuel-rich conditions (ϕ = 1.4 - 2.0) and a cooler temperature (1350°C). For completeness, the reactor was also run at one fuel-lean condition (ϕ = 0.7). To enhance sensitivity for PIC measurement, a novel analytical approach involving a microtrap (Mitra et al. 1995) was utilized.

For all modeling efforts, the FORTRAN package CHEMKIN (Kee et al. 1986) was used to simulate the PSR + PFR sequence. To model the initial experimental work, a total of four different chemical reaction mechanisms were used to validate the reactor and determine the effectiveness of each. The best fitting mechanism was then applied to the second series of runs. In order to predict the experimental PIC formation, an aromatic mechanism was also applied to the fuel-rich runs.

CHAPTER 2

LITERATURE SURVEY

Considerable combustion research has been focused on two related areas - mixing constraints and PIC production. A representative sample of these efforts is presented here. Because PIC production is enhanced by chlorocarbon combustion, relevant sample chlorine publications have also been included.

The concept of incomplete mixing is not new. Hottel et al. (1967) studied the flow configuration and mixing patterns with a toroidal jet-stirred reactor. They then utilized this information to predict the effects that such flow patterns would have on overall reactor performance. Since the publication of this work, the mixing problem has been the focus of much research including Longwell et al. (1989), Tonouchi et al. (1994), and Wendt (1994).

Longwell et al. (1989) noted that within a well stirred combustor, some reactions can be faster than the mixing process. Such a reactor would require modeling of the turbulent mixing. A comparison between fuel-lean CO/H_2 combustion and fuel-rich C_2H_4-air combustion demonstrated this idea. Because the CO/H_2 reactions are fast, it was shown to be important to take the jet mixing nature of the flow into account. For the slower ethylene reactions, the simple ideal perfectly stirred reactor (PSR) assumption was sufficient.

Because all practical combustion devices experience both macro- and micro-mixing to some degree, Tonouchi and co-workers (1994) chose three models which allowed for independent control of the rate of macromixing and micromixing.

Comparing the modeled results with their experimental database of methane-air fuel-lean combustion, Tonouchi et al. concluded that the success of each model was directly dependent on the reactor loading. At high loading levels, the reactor is well macromixed and micromixed and can be accurately modeled. While at low levels, the reactor is not mixed consistently and therefore good agreement could not be achieved using current models.

Wendt (1994) spoke about the need for understanding both the physical processes and chemical kinetics during combustor failure modes because the most harmful organic emissions occur during these disturbances. By accurately simulating turbulent reactive flows and mixing, a better understanding of turbulent fluctuations, as opposed to turbulent mean flows, can be obtained.

Production of PICs is enhanced by the combustion of inhibitory compounds, as well as by incomplete mixing. Chlorinated compounds are known to inhibit hydrocarbon combustion. This inhibition has been the focus of much research in recent years. Current joint research between NJIT and MIT continues with a similar theme. One of the objectives is to gain a better understanding of both mixing constraints and PIC production, especially with the addition of chlorine into the system. As described in the Introduction, since non-premixed fuel-lean chlorocarbon combustion produces elevated PIC levels, especially aromatics, there must be fuel-rich pockets and therefore fuel equivalence ratio faults within the system.

Barat et al. (1990) and Brouwer et al. (1992) utilized a toroidal jet stirred combustor (TJSC) to incinerate chlorinated and non-chlorinated species. Using the perfectly stirred reactor (PSR) model and the measured probability density functions

(PDFs) of instantaneous temperatures, Barat et al. (1990) found that under fuel-lean conditions, the addition of chlorine resulted in localized combustion instabilities. Modeling of the reactions indicated that chlorine primarily destabilizes by inhibiting CO burnout. The two reactions

$$OH + HCl = H_2O + Cl$$

$$Cl + HO_2 = HCl + O_2$$

both successfully reduce the OH radical necessary for CO burnout by $CO + OH = CO_2 + H$. Under fuel-rich chlorinated conditions (Brouwer et al., 1992), the chlorine-inhibited CO burnout was again observed. Once again, the HCl consumption of OH was found to be the primary cause. In addition, HCl molecules readily react with H and O radicals to produce the Cl radical. Increased levels of intermediate hydrocarbons, oxygen, and CO were observed.

Recent work performed on a two staged combustor at MIT (Brouwer et al. 1994) focused on both the incomplete mixing and chemical kinetic constraints which affect the formation of PICs. Methyl chloride (CH_3Cl) was injected near the inlet of the second stage. The PIC (e.g. benzene) production near the injection point was greater than farther down the reactor. This demonstrates the effect of poor mixing. In addition to the mixing constraint, the chemical kinetic constraints were demonstrated during this research as well. Along the length of the second stage, the hydrocarbon burn-out was more rapid than the CO burnout, indicating that relative kinetic rates are a major constraint on combustion as well.

Although chlorine enhances PIC production, under certain conditions hydrocarbon combustion alone will yield undesirable products. Since this thesis contains ethylene/air runs only, the following articles are appropriate since each research group uses the same fuel source.

Using a jet-stirred combustor, the same as in this thesis, a group from MIT (Vaughn et al. 1991) studied the fuel-rich combustion of ethylene (C_2H_4) and air. The concentrations of the major stable species were found to agree quite well with a model consisting of a single perfectly stirred reactor (PSR) and a reaction mechanism proposed by Glarborg, Miller, and Kee (1986). Probe quench calculations were also performed. At low equivalence ratios (1.3 - 1.5), significantly better agreement is achieved with the addition of the probe calculations. This is because there are many more radicals at the lower equivalence ratios. At ratios above 1.5, the effects of probe quenching are diminished due to the smaller radical concentrations relative to the concentrations of the major stable species.

Lam, Howard, and Longwell (1990) utilized the same two stage reactor to combust ethylene at a fuel equivalence ratio of 2.18. To enhance the production of polyaromatic hydrocarbons (PAHs), tar, and soot, some of the fuel in the form of ethylene or benzene was injected between the two reactor zones. The injection of ethylene into the second stage resulted in a high conversion to C_2H_2 as well as benzene and PAHs, while the benzene addition greatly enhanced the production of tar and soot. Lam et al. concluded: 1) that C_2H_2 may have added to the mass of the tar inventory, and 2) that the mechanisms for PAH formation should include acetylene addition reactions

and oxidation reactions. The importance of acetylene to higher molecular weight growth is clearly demonstrated by this research.

Additional proof of the importance of the acetylene precursor for molecular weight growth to PAH and soot is offered by Smedley and co-workers (1992). Smedley et al. performed an ethylene/air study of soot formation and deposition utilizing a flat-flame, water-cooled, premixed burner. Although the thrust of the work was on the role of PAH species, the importance of acetylene (C_2H_2) on soot particle inception was considered as well. It was determined that PAHs are probably more extensively involved in soot particle inception than previously believed. The acetylene, on the other hand, is not thought to be directly involved in soot particle inception, but is more involved in sustaining soot growth after the PAH species are depleted. It was also shown that PAH growth via C_2H_2 addition at radical sites is possible. Even though the effects of acetylene were not as pronounced as anticipated, it remains a major precursor to higher molecular weight growth.

CHAPTER 3

EXPERIMENTAL APPARATUS

The experimental apparatus can be divided into four sections: the feed system, the two-staged reactor, the sampling system, and the analytical system. The overall schematic is shown in Figure 3.1. Other relevant corresponding schematics are included where appropriate.

3.1 Feed System

In order to control the flow of each gas, it is first regulated to a desired pressure and then flowed into a rotameter. The rotameter flowrates are corrected as needed for molecular weight, pressure, and temperature using the following equation.

$$V_A = V_C \sqrt{\left(\frac{P_A}{P_C}\right)\left(\frac{T_C}{T_A}\right)\left(\frac{W_C}{W_A}\right)}$$

where P is pressure in psia, T is temperature in Kelvin, W is molecular weight, V is volumetric flow rate in STP (20°C and 14.7 psia) units. The subscripts A and C are actual conditions and calibration conditions, respectively. After metering, all the gases are teed into a main feed manifold which is fed to the first stage of the reactor. (See Figure 3.2.)

Ethylene (C_2H_4) is the primary fuel and is supplied by Matheson Gas Products, Inc. It is 99.99% polymer grade purity. Two cylinders of ethylene are used in parallel.

Ethylene at cylinder pressure is flowed through a hot water bath before the regulator in order to compensate for Joule-Thomson cooling which occurs as a result of the pressure drop across the regulator. After preheating and regulating to 80 psig, the C2H4 temperature is typically 20°C which is a desirable feed temperature.

High pressure air from an in-house compressor is used as an oxidant. A knock-out filter is mounted on the air line to remove any oil particles and saturated moisture from the air. The air is regulated to 80 psig prior to its rotameter.

Methylene chloride (CH_2Cl_2) will be used in future work to simulate chlorinated hazardous wastes. It was purchased as a liquid from Fisher Scientific, Inc. An atomizer/vaporizer unit was constructed to feed the CH_2Cl_2 as a gas. (See Figure 3.3.) Propellant nitrogen and metered liquid CH_2Cl_2 are flowed through a nozzle which sufficiently atomizes the liquid. Directly following the nozzle, there is a 12" heater which vaporizes the atomized spray. The gaseous CH_2Cl_2 then flows through a heat traced ¼" line which tees into the main feed manifold near the entrance to the reactor.

3.2 Two-Stage Reactor

The system used for this research is an atmospheric pressure, small pilot-scale two-stage combustion chamber. (See Figure 3.4.) The first stage of the reactor is a 250 cm^3 toroidal zone constructed of castable high temperature alumina. Gases enter the zone at sub-sonic velocities through 32 jets angled 20° off radius, thereby producing highly turbulent swirling and intense back-mixing. Since the first stage has been shown to simulate perfectly stirred reactor (PSR) behavior under most normal conditions

(Nenninger 1983; Lam 1988; Barat 1990; Vaughn et al. 1991; Barat 1992; Mao 1995), it is hereby referred to as the PSR zone.

Combustion gases flow out of the first zone, through a ceramic flow straightener, and into the second zone. Because additional air or steam is often desired in the second zone, a ceramic injector is placed in between the two zones. The necessary gases are metered and flowed into the system via the injector. The second zone is constructed from a precast alumina tube, 30 centimeters in length and 5 centimeters in diameter. Since the second stage has been shown to simulate plug flow reactor (PFR) under most conditions, (Lam 1988; Mao 1995) it is hereby referred to as the PFR zone.

To reduce heat losses from the reactor, both stages are encased with alumina-based insulation and enclosed in stainless steel jackets. The exterior jacket of the PFR zone is covered with fiberglass insulation as well. The hot gases then enter the afterburner section, which is lined with a stainless steel annular region through which coolant is flowed. To consume unburned species and help further cool the exhaust gas, a large volume of air is injected into the afterburner section. Cooling water is sprayed on the afterburner flue gases before venting.

3.3 Sampling System

The sampling system is shown Figure 3.5. Within each zone of the reactor, there is a liquid-cooled stainless steel probe. The PSR probe is stationary, while the PFR probe can be moved axially in order to measure concentration as a function of residence time. For this work, the PFR probe remains at the exit of the PFR zone. Combustion gases are drawn through these probes by use of a metal bellows pump. The coolant used in the

probes is an approximately equal volume of ethylene glycol and water available from an in-house supply. Before the coolant is flowed through the probes, it first flows through the annular heat removal zone of the afterburner. By controlling the coolant flowrate, its temperature can be raised from 15°C to 40 - 50°C. While this temperature is cool enough to maintain the probe integrity and quench the combustion gas sample, it is sufficiently warmer than the HCl acid dew point of the combustion gas. If chlorinated compounds are burned, the gases are directed through an oversized counter-current scrubber which essentially removes all HCl in the sample gas. The sample line between the probe and the scrubber is heat traced to maintain the warm temperature. The gas is then directed through a cooler, then a water knock-out, and then the metal bellows pump. From the pump, gases are pushed into the analytical devices available near the reactor.

3.4 Analytical System

The analytical system is shown in Figures 3.6, 3.7, and 3.8. Once the combustion gases have been drawn from the reactor, scrubbed thoroughly, and dried, the gases can then be routed to go through one of five continuous emission monitors (CEMs) available on-line: oxygen, carbon monoxide, carbon dioxide, nitrogen oxides, and total hydrocarbons. For this work, only the oxygen CEM was utilized with significant frequency.

Besides the CEMs available, the gases can also be directed to either a Hewlett-Packard 5890 Series II or a Varian 3400 gas chromatograph. The HP GC has two columns (Columns A and B) and the Varian has only one column (Column C). All three columns are equipped with flame ionization detectors (FIDs). The signal peaks from the

HP FIDs are recorded and integrated by a Hewlett Packard 3396 Series II Integrator, while the signal peaks from the Varian FID are recorded and integrated by a HP 3395 Integrator. To calibrate the columns, the GC sample loops were evacuated using a vacuum pump, and then static filled with a standard gas to the same pressure as used for the combustion samples. The specifics of each standard are included in Appendix B.

The first column, Column A, is a Heliflex AT-1 capillary column, 30 m × 0.53 mm × 5μm. This column was chosen in order to detect trace amounts of volatile organics existing in the emission gases. Prior to entering this column, combustion gases are flushed through a heated (80°C) 10 ml copper tubing loop connected to a six port gas sample valve. Upon injection, the sample loop is then flushed with 3 ml/minute of carrier helium for four minutes. In order to concentrate the sample to enhance sensitivity for low level PICs, it is flowed through a microtrap (Mitra et al. 1995). The microtrap used for this chromatography was made using a 14 cm × 0.53 mm silica lined stainless steel tube packed with 60 mesh Carbotrap C. After briefly heating the trap with 25 Volts for 1.0 second to affect desorption, the concentrated slug of gas is then pushed into the column. The GC oven is ramped from 10°C to 200°C at 5°C/minute in order to sufficiently separate the desired trace compounds.

The second column, Column B, is a 1.0 m AT-1000 and is utilized to detect light hydrocarbons, such as methane, ethane, ethylene, and acetylene. Nitrogen at a flowrate of 30 ml/minute is the carrier gas. The sample gas is flushed through a heated 1 ml six port gas sample valve. Upon injection, the loop is flushed with the nitrogen carrier.

After injecting the sample, the GC oven is held at 35°C for one minute, ramped at 5°C/minute until reaching 45°C when it is held constant for one additional minute.

Because the sensitivities for both the carbon monoxide and carbon dioxide meters were not adequate at the time of this study, the Varian GC was utilized specifically for determining the desired carbon oxide levels. Light hydrocarbons can also be seen with the Varian column, Column C. Although CO and CO_2 are the compounds of concern, light hydrocarbon measurements were taken for verification. The GC is equipped with an FID and an 1/8" column packed with Carbosphere. Once again, the combustion sample gas is flushed through a 1 ml six port sample valve prior to injection to the column. Since an FID cannot detect the carbon oxides, the separated sample gases, along with excess hydrogen, are first routed through a heated (300°C) ruthenium catalyst converter which reduces the carbon monoxide and carbon dioxide to CH_4, which is quite detectable by the FID.

CHAPTER 4

MODELING METHODS

There are two segments to the modeling of this work - reactor simulation and reaction mechanism.

4.1 Reactor Simulation

As discussed in the Experimental Methods, the jet-stirred primary zone of the two-stage combustor can be simulated as a perfectly stirred reactor (PSR) under most conditions (Nenninger 1983; Lam 1988; Barat 1990; Vaughn et al. 1991; Barat 1992; Mao et al. 1996). Departure from PSR behavior can occur at elevated feed flow rates and lower temperatures (Barat 1990, 1992). For all of the experiments performed in this study, PSR behavior was maintained since only moderate feed flow rates and a high first stage temperature were used. The linear flow second zone allows for little axial mixing, it can be simulated as a plug flow reactor (PFR) (Lam 1988; Mao et al. 1996).

In order to simulate the PSR + PFR reactor, the general purpose CHEMKIN chemical kinetics package (Kee et al. 1986) is used. To access the many subroutines within the CHEMKIN package, an application driver code (reactor simulation) is needed. For this work, the driver code created by Mao (1995) was used. This driver accesses the CHEMKIN PSR code (Glarborg et al. 1986) and the ordinary differential equation solver, LSODE (Hindmarsh 1983) for the PFR. Note that for K total species, there are K species balance equations for each zone. The governing species balance equations for the PSR are:

$$M(Y_k - Y_{ko}) = \omega_k W_k V$$

where M is the mass flow rate, Y_k is the mass fraction of species k, Y_{ko} is the inlet mass fraction of species k, ω_k is the net molar rate of production by reaction of species k, W_k is the molecular weight of species k, and V is the reactor volume. The governing species balance equations for the PFR are:

$$\frac{dY_k}{dt} = \frac{\omega_k W_k}{\rho}$$

where t is the reaction time and ρ is the mass density of the combustion gases.

A corresponding enthalpy balance can be written for each reactor zone. However, these are not required since observed reactor temperature data are input to the driver program.

The driver computer code requires the following information; the feed compositions and flow rate, the measured temperatures in both stages, either the PSR volume or residence time, the reactor pressure, and the PFR residence time. PFR temperatures are inputted as either a quadratic (Mao 1995) or a cubic equation. For approximately half of this research, the second stage had three thermocouples. An additional thermocouple was later added to better simulate the PFR temperature profile. All second stage temperatures were regressed using the method of least squares and the appropriate equation form. Both general equations are shown below.

$$T_{PFR} = A + B\tau + C\tau^2$$

$$T_{PFR} = A + B\tau + C\tau^2 + D\tau^3$$

where T_{PFR} is the temperature in Kelvin, the constants A, B, C, and D are regressed parameters, and τ is the residence time in the PFR. The residence time was calculated using the following equation.

$$\tau = \frac{\Delta V}{R \times M \times T_{ave}}$$

where ΔV is the incremental volume, R is the ideal gas constant, M is the inlet number of moles per second, and T_{ave} is the average temperature within the volume, ΔV. Since the existing reactor computer code (Mao 1995) only allowed for quadratic equations, it was modified to allow input of the fourth constant. Figure 4.1 shows a typical cubic temperature profile. The line is the regressed temperature profile, while the individual points are the measured experimental values.

The driver computer code also allows for modeling of air and/or steam staged combustion work. The injection material, temperature, composition, and flow rate must be supplied. Although not used for this work, this particular code can also perform rate-of-production, sensitivity, and probe quench calculations.

4.2 Reaction Mechanism

In conjunction with the reactor simulation, a detailed elementary reaction mechanism is necessary to generate the species net reaction rate ω_k. A reaction mechanism consists of a set of reversible elementary gas phase chemical reactions and a species thermodynamic property set. Provided with each reaction is the forward kinetic rate constant, k_{fi}.

$$k_{fi} = A_i T^{ni} \exp\left(-\frac{E_i}{RT}\right)$$

where A_i, n_i, and E_i are parameters specific to the i^{th} reaction. The reverse rate constant k_{ri} is related to the forward rate constant through the reaction equilibrium constant, K_i.

$$k_{ri} = \frac{k_{fi}}{K_i}$$

In order for CHEMKIN to calculate the needed equilibrium constant K_i, a complete set of thermodynamic data consisting of standard heats of formation, entropies, and heat capacities as a function of temperature for each species must be supplied by the user.

The reaction mechanisms (reaction set plus species thermodynamics) used for the modeling are drawn from literature. A set of four mechanisms was used as a basis of comparison for the Reactor Validation section. The mechanisms are taken from Barat (1990), Ho et al. (1992), Chiang (1995), and Mao (1995). In an effort to characterize the

interaction of turbulent mixing and chemical reaction within a toroidal jet-stirred combustor, Barat (1990) utilized the C_1/C_2 hydrocarbon oxidation reactions within the Miller/Bowman mechanism (1989). To make the mechanism more consistent with experimental conditions within the reactor, Barat modified selected reactions and parameters using Quantum-Rice-Ramsberger-Kassel (QRRK) method (Dean 1985). The Ho mechanism was extracted from a larger mechanism (Ho et al. 1992) which included chlorinated species. This chlorinated mechanism was used to model the pyrolysis and oxidation of chloromethanes. The Chiang mechanism (1995) also focuses on chloromethane. The emphasis of this mechanism is the growth of chlorinated aromatic precursors. The Mao mechanism (1995) was created to model a series of air and steam staged combustion runs with methyl chloride and methyl amine doping. The C_1/C_2 portion of the Mao mechanism was taken from Ho (1993). QRRK was used to modify selected reactions.

The focus of the second part of this research effort was on the production of the PIC benzene. The Zhong mechanism (Zhong et al. 1996) was used for modeling. This particular mechanism incorporates 1,3-cyclopentadiene since it has been found to be an important intermediate in the oxidation and decomposition of aromatic species (Lovell et al. 1988, Brezinsky et al. 1990). It also incorporates sufficient hydrocarbon species to allow for molecular weight growth from ethylene to benzene.

Since this research involves only hydrocarbons, all chlorine and nitrogen reactions within each mechanism have been removed. Each of the above described mechanisms

has its corresponding thermodynamic file to which it is linked. The resulting link file is then used by the CHEMKIN code to determine the net chemical production rate ω_k.

CHAPTER 5

REACTOR VALIDATION

5.1 Introduction

Upon completion of the staged combustion work of Mao in December 1994, the combustor was completely rebuilt. All castable alumina reactor components and all insulation were replaced. A number of modifications were made on the existing system. Two new afterburner sections with cooling water jackets were added to allow for improved heat recovery and integration. A fourth PFR thermocouple was added between the PSR exit and the first existing PFR thermocouple. Although liquefied methylene chloride was not used during this work, an atomizer/vaporizer unit was constructed and tested.

For the purposes of system testing and validation after the overhaul, a series of runs with ethylene and air under various feed conditions were made in the two-stage combustor. These runs included both fuel-lean (excess air) and fuel-rich (excess fuel) conditions. Species concentrations and reactor temperatures were measured in all runs. In order to verify that the reactor was indeed behaving as a PSR followed by a PFR, detailed modeling of these with known reaction mechanisms was performed on the fuel-lean and fuel-rich cases. Comparisons were made of the observed species concentration data with the model predictions.

The feed condition is characterized by the fuel equivalence ratio, which is defined as the actual fuel to air ratio divided by the stoichiometric fuel to air ratio. The general equation for equivalence ratio, ϕ is

$$\phi = \frac{\left(F/A\right)_{actual}}{\left(F/A\right)_{stoich.}}$$

where F are the volumetric or molar flow rates of fuel in the feed mixture and A are the volumetric or molar flow rates of air in the feed mixture. For fuel-lean systems, ϕ is less than 1, while for fuel-rich systems, ϕ is greater than 1. At stoichiometric conditions, ϕ equals 1.

The stoichiometric condition is determined based on the assumption of complete combustion to the most thermodynamically stable products. In the case of ethylene combustion, the global stoichiometry is:

$$C_2H_4 + 3O_2 \rightarrow 2H_2O + 2CO_2$$

Using this reaction in conjunction with the general equation for ϕ, one can obtain the equivalence ratio equation in terms of the actual air and ethylene flowrates:

$$\phi = \frac{3}{0.21}\left(\frac{Ethylene}{Air}\right)_{actual}$$

Often, dilution nitrogen is added with the feed to control the PSR temperature. Under fuel-lean conditions, the large amount of nitrogen carried by the combustion air serves as a heat sink. Under fuel-rich conditions, this heat sink is not available due to the considerably lower amount of feed air; hence, dilution nitrogen is required. In an effort to make the PSR temperatures as consistent as possible, most conditions both fuel-lean and fuel-rich required the dilution nitrogen. Although the additional nitrogen affects the feed compositions and total flowrate, it does not influence the equivalence ratio.

5.2 Stable Species Analysis of C_2H_4/Air Combustion

The first motivation of this work has been to validate the PSR + PFR reactor sequence. In order to do so, the two staged combustion chamber was run at seven different fuel equivalence ratios, ranging from fuel-lean to fuel-rich. To make the conditions consistent, the appropriate amount of nitrogen was added to the reactor to maintain a first stage temperature of 1450°C. The experimental conditions are included in Table 5.1. Combustion samples were taken from both the first and second stage. For this part of the research effort only the concentrations of CO, CO_2, O_2, and light hydrocarbons were found.

The validation of the reactor as a PSR + PFR depends partly on the goodness of the mechanism used. As mentioned in the Chapter 4.0, four mechanisms (Barat 1990, Ho et al. 1992, Chiang 1995, and Mao 1995) were tested. While each had been used previously for various applications, a head-to-head comparison has not been done to date. If a good

fit to the experimental data can be obtained using a proven mechanism, then the reactor is declared validated for use on future studies.

Table 5.1 - Inlet Conditions for Reactor Validation

	Fuel Equivalence Ratio (ϕ)	Inlet Mole Fraction	Inlet Mass Flowrate (g/sec)
Condition 1	0.594	N_2 - 0.759 O_2 - 0.202 C_2H_4 - 0.040	5.950
Condition 2	0.692	N_2 - 0.787 O_2 - 0.173 C_2H_4 - 0.040	6.573
Condition 3	0.794	N_2 - 0.806 O_2 - 0.153 C_2H_4 - 0.040	6.940
Condition 4	0.916	N_2 - 0.832 O_2 - 0.128 C_2H_4 - 0.039	7.780
Condition 5	1.190	N_2 - 0.836 O_2 - 0.117 C_2H_4 - 0.047	7.500
Condition 6	1.347	N_2 - 0.817 O_2 - 0.126 C_2H_4 - 0.057	6.520
Condition 7	1.540	N_2 - 0.793 O_2 - 0.135 C_2H_4 - 0.069	5.570

The experimental and modeling results from the first stage are shown in the odd-numbered figures, while the results from the second stage are shown in the even-numbered figures. Each species is presented on its own graph to clearly show both the experimental and the modeling results.

As seen in Figures 5.1 and 5.2, the experimental CO levels in the PSR and PFR are very low under fuel-lean conditions. This is a result of the CO burn-out phenomenon

which occurs readily in oxygen-rich combustion. When the CO is made, it is quickly converted to CO_2. There is slightly less CO in the PFR than in the PSR under fuel-lean conditions. This is because the small amount of CO leaving in the backmixed first stage is readily converted to CO_2 in the plug flow environment of the second stage. Once the system is run fuel-rich, the CO levels quickly increase. There is no longer any oxygen to continue with the CO conversion to CO_2. The CO levels are very similar in both zones under fuel-rich conditions since the limiting reagent oxygen is effectively exhausted in the PSR. Because there is little to no oxygen, the CO molecule is fairly stable in this second zone and therefore its concentration does not vary greatly.

Figures 5.3 and 5.4 depict the CO_2 concentrations within each zone. The fuel-lean results show a gradual downward slope, while the fuel-rich conditions show a markedly steeper slope. This decrease in CO_2 arises because of the decrease in oxygen within the system. As the fuel equivalence ratio is increased, the mole fraction of oxygen within the system is decreased.

The oxygen levels within the PSR and the PFR are shown in Figures 5.5 and 5.6. As expected, the oxygen concentration decreases as the fuel equivalence ratio increases from fuel-lean to stoichiometric conditions. Figures 5.7 through 5.10 show the methane and acetylene concentrations. In a system with excess oxygen, almost all of the ethylene is combusted to stable products. Fuel-rich conditions, on the other hand, are conducive for light hydrocarbon existence and molecular weight growth.

5.3 Comparison with Modeled Results

All of the figures show that the four mechanisms modeled the experimental results closely under fuel-lean conditions. Major modeling discrepancies do arise under fuel-rich conditions, especially for the Chiang mechanism.

In order to know the certainty of the experimental results, a carbon balance was performed around the combustor. Figure 5.11 shows the comparison between the inlet and outlet carbon mole fraction. The percent difference varies from 9.7% to 17.4% with an average deviation of 13%. In all conditions, the outlet carbon content exceeded the inlet carbon content. This offset resulted from a discrepancy either on the inlet C_2H_4 flowrate or in the analysis of the carbon-containing products, or both. Since there is no conclusive source for the error, no corrections were made. Instead the average deviation has been added to all experimental points in the form of error bars.

As seen on the fuel-lean end of Figure 5.1, three out of four models overpredict the CO experimental levels by a factor of three. Since the CO levels are so low at these oxygen rich conditions, any modeling deviations are amplified greatly. The fuel-lean end of Figure 5.2 shows that both experimental and modeled results lie on top of one another on the current scale. Under fuel-rich conditions, for the most part, the models underpredict the experimental results from both zones. The Chiang mechanism, on both charts, is especially far removed from the data, while the Barat and Mao mechanisms model the results the closest. At the highest fuel equivalence ratio ($\phi = 1.54$), the percent differences between the Chiang, Ho, Barat, and Mao mechanism and the experimental results are 78%, 38%, 22% , and 21%, respectively.

The modeling of CO_2 concentrations in Figures 5.3 and 5.4 show good agreement throughout the varying fuel equivalence ratios. In both zones, the majority of the CO_2 concentrations were predicted within the presumed error of 13%. In the PSR (Figure 5.3), the Chiang model lies closest under fuel-lean conditions, while the Ho mechanism models the best under fuel-rich conditions. Figure 5.4 shows all four mechanisms modeling the fuel-lean experimental PSR results within 6%. Under oxygen-starved conditions, the Ho mechanism once again modeled the closest. In general, most model predictions fell below the experimental data with the exception of the Chiang mechanism which under fuel-rich conditions deviates from the CO_2 trend in each zone. Instead of progressing downward like both the experiment and the other models, the Chiang mechanism either levels out (in the PFR) or increases slightly (in the PSR).

Experimental and modeled oxygen levels follow the same trend, especially under fuel-lean conditions. In both the PSR (Figure 5.5) and the PFR (Figure 5.6), all of the mechanisms modeled the experimental levels within an average of 12%. Major deviations only occur under fuel-rich conditions within the PSR. Here, the Chiang mechanism overpredicts the oxygen level by a factor of three (ϕ = 1.54) to four (ϕ = 1.19). Other than this divergence, the remaining modeled results consistently, but only slightly underpredict the experimental results.

Since the light hydrocarbon concentrations are significantly lower than the CO, CO_2, and O_2 levels, the small deviations between each model are more apparent. Each follows the expected upward trend with the increase of equivalence ratio, but all overpredict the experiment. The CH_4 figures (Figures 5.7 and 5.8) show that the Barat

mechanism predicts the best, while the C_2H_2 figures (Figures 5.9 and 5.10) show that both the Mao and Barat mechanisms equally predict the closest. In both cases, the Chiang mechanism greatly exceeds the experimental results.

5.4 Preferred Mechanism

The focus of the work to this point has been to validate the reactor as a PSR+PFR and to compare the modeling ability of four different C_1/C_2 hydrocarbon mechanisms. The validation of the reactor as a PSR+PFR depends partly on the goodness of the mechanism used. Although the percent deviations varied from species to species, the Barat and Mao mechanisms were shown to best agree with the experimental results overall. The Ho mechanism was slightly less successful, while the Chiang mechanism demonstrated the largest deviations from the experimental data. There is a possible explanation for the significant discrepancies between the experimental results and the Chiang model. The combustor was run at conditions (high fuel equivalence ratios) at which molecular weight growth occurs. Since the Chiang mechanism is the only mechanism of the four which includes this growth, it should have modeled the experimental data the best. Since it did not, perhaps the Chiang mechanism lacks good C_1/C_2 chemistry. Although the Ho and Chiang mechanisms did closely model some portions of the experimental results, the Barat and Mao mechanisms were by far the most consistent. Since the Mao mechanism is more recent, it is the preferred mechanism and will be applied to the stable species measurements in subsequent work presented in Chapter 6.0.

Within the accuracy of the data, the Mao mechanism has successfully proven that the reactor is a PSR+PFR sequence. This mechanism has been validated previously using

the same reactor facility. While the discrepancies between experiment and model vary slightly between the Mao results (Mao 1995) and the results of this work, the two arrive at the same conclusion that the two stage turbulent flow combustor is indeed a PSR, followed by a PFR.

CHAPTER 6

FUEL-RICH COMBUSTION OF C_2H_4/AIR

6.1 Introduction

The second section of this research focuses on the post-reactor validation fuel-rich combustion of ethylene and air with nitrogen as the diluent for first stage temperature control. One fuel-lean condition was also performed for completeness. The experimental conditions are listed in Table 6.1. For all runs, the appropriate amount of dilution nitrogen was added to make the PSR temperature equal to approximately 1350°C.

Table 6.1 - Inlet Conditions for Fuel-Rich Runs

	Fuel Equivalence Ratio (ϕ)	Inlet Mole Fraction	Inlet Mass Flowrate (g/sec)
Condition 1	0.693	N_2 - 0.801 O_2 - 0.162 C_2H_4 - 0.037	7.510
Condition 2	1.387	N_2 - 0.828 O_2 - 0.117 C_2H_4 - 0.054	6.807
Condition 3	1.578	N_2 - 0.807 O_2 - 0.126 C_2H_4 - 0.066	6.238
Condition 4	1.786	N_2 - 0.785 O_2 - 0.135 C_2H_4 - 0.080	5.571
Condition 5	1.935	N_2 - 0.771 O_2 - 0.139 C_2H_4 - 0.090	6.115

Sample gases were taken from the PFR exit only. The concentrations of light hydrocarbons, CO_2, CO, and O_2 were determined. The microtrap was also used to analyze the amount of higher molecular weight compounds present within the combustion gases. Problems were encountered, to be briefly discussed in Section 6.3, in the use of the trap under fuel-rich conditions. Only benzene was quantified within the microtrap samples. However, qualitative discussion of the other observed GC peaks is included.

As a result of the conclusions made in Chapter 5.0, the Mao mechanism (Mao 1995) was chosen for subsequent modeling. Because the mechanism includes no molecular weight growth, only CO_x, O_2, CH_4, and C_2 hydrocarbon species were successfully modeled using this mechanism. Since the Zhong mechanism (Zhong et al. 1996) includes aromatics - namely benzene, it was used to model the experimental results in this chapter as well.

6.2 Experiment and Model Results of Fuel-Rich Combustion

Figures 6.1 through 6.4 show the carbon monoxide, carbon dioxide, methane, and acetylene concentrations - both experiment and model - as a function of fuel equivalence ratio. Figures 6.5 and 6.6 provide the benzene results. On the semi-logarithmic graphs (Figures 6.3, 6.4, and 6.6), the one fuel-lean condition is not included since the experimental levels are lower than the sensitivity of the analytical equipment (and are therefore assumed to equal zero). Since zero cannot be shown on a logarithmic scale, it has been omitted on the graphs in question. The oxygen results have not been graphed

because the majority of the conditions are fuel-rich. Thus little to no oxygen survives to the PFR exit. Both modeling and the observed oxygen levels are consistent with this fact.

There is good agreement between the Mao mechanism and experiment for both CO and CO_2 (Figures 6.1 and 6.2). Slight CO deviations occur at the higher fuel equivalence ratios, while the CO_2 levels are closely aligned. The Zhong mechanism models the fuel-lean condition closely for both CO and CO_2, but deviates sharply under fuel-rich conditions. The deviation between the Zhong model and CO concentration increases from 55% at ϕ = 1.387 to 66% at ϕ = 1.935, while the deviation between model and CO_2 concentration decreases from 71% at ϕ = 1.387 to 20% at ϕ = 1.935.

The light hydrocarbons are shown in Figures 6.3 and 6.4. Because the reactor was run at very fuel-rich conditions, both GC columns B and C were able to read the methane and acetylene levels. For this reason, two experimental points are presented for each fuel equivalence ratio. In all cases, the two lie close to one another, thus verifying the validity of the experimental results. Since the Zhong model significantly underpredicts the experimental results, the fuel-rich hydrocarbon data is shown on semi-logarithmic paper.

For all but the lowest fuel-rich condition (ϕ = 1.387), the Mao mechanism slightly overpredicts both the CH_4 and C_2H_2 levels. At ϕ = 1.387 though, the model exceeds the experiment by a factor of twenty for each species. At the higher equivalence ratios (ϕ = 1.578 - 1.935), it is likely that more light hydrocarbons are linking and forming the higher molecular weight species. The Mao mechanism does not include molecular weight growth; therefore the model predicts elevated concentrations of light hydrocarbons. The Zhong mechanism, on the other hand, includes molecular weight growth and therefore

should model the results more closely. Better agreement was not achieved. The CH_4 levels (Figure 6.3) differ by approximately three orders of magnitude, while the C_2H_2 levels (Figure 6.4) differ by more than one order of magnitude.

Due to difficulties encountered in the microtrap analytical work, benzene (retention time = 19.4 minutes) was the only product of incomplete combustion (PIC) quantitatively identified. The benzene results are provided in Figures 6.5 and 6.6. Figure 6.5 shows only the experimental benzene levels. As seen on Figure 6.5, at an equivalence ratio of about 1.5, the benzene levels begin to rise sharply. Coincidentally, C_2H_2 also rises fairly well at ϕ of 1.5. (See Figure 6.4.) Acetylene is a well known precursor to benzene in fuel-rich combustion (e.g. Lam et al. 1990). Similar benzene concentrations have been seen by Lam and his co-workers (1990) using the same system design and same fuel source. At a fuel equivalence ratio of 2.18, the benzene concentration in the Lam PFR was recorded to be approximately 200 ppm which is in-line with the current experimental results.

As mentioned previously, the Zhong mechanism alone was used to model the benzene levels. Figure 6.6 shows the model and experiment on a semi-logarithmic scale. Similar to the experiment, the model predicts an increase in benzene concentration as a function of equivalence ratio, but the deviations range from a factor of 1.5 (ϕ = 1.387) to a factor of 30 (ϕ = 1.935).

Comparing the two mechanisms, the Mao model was far more successfully when applied to the CO_x and light hydrocarbons. For all measured species, the Zhong mechanism failed to accurately model the experimental results, though it did follow the

experimental trend of increased hydrocarbon concentrations with increased equivalence ratios. It is possible that the Zhong mechanism, like the Chiang mechanism used in Chapter 5.0, lacks an adequate light hydrocarbon base.

6.3 Qualitative Discussion of Other Integrated Peaks

The GC method used with the microtrap resulted in generally poor chromatography as applied to date in this work. (See Figure 6.7.) It is generally felt (Mitra 1996) that the high sensitivity (e.g. ppb) afforded by the microtrap used in conjunction with a capillary column was simply swamped by the high levels of hydrocarbons collected from the fuel-rich runs. It has been suggested (Mitra 1996) that better chromatography would be possible with a much reduced sample loop volume (e.g. 1 ml). As a result, only qualitative results are presented here for all GC integrator results. There is little doubt that these responses from the GC flame ionization detector represent hydrocarbons.

Although the microtrap prior to column A provided very little definitive results, much can be said qualitatively about the four fuel-rich chromatograms. In an attempt to make tentative and general identifications, three charts were generated with respect to varying retention time periods. These retention time periods were chosen in an attempt to group together peaks which were closest together as reported by the GC integrator.

Figures 6.8 and 6.9 show the summation of areas within the six chosen time periods as a function of equivalence ratio. The x-y chart shown in Figure 6.8 clearly demonstrates the expected trend of increased hydrocarbons with increased equivalence ratio, especially for the 4-6, 7-9, and 16-20 minute time intervals. Figure 6.9 shows the same information using a three dimensional bar graph. This format allows for better

comparison between the experimental and standard results. Figure 6.10 shows area summation from a standard which includes the six normal alkanes from methane (C_1) to hexane (C_6), and was analyzed with the GC via the microtrap method used for the combustion samples. Although the standard contained six species, only four significantly sized groups were found. This leads one to conclude that more than one species has been included in some of the groups.

The two bar charts (Figures 6.9 and 6.10) overlap significantly for three time increments: 4-6 minutes, 7-9 minutes, and 16-20 minutes. On the basis of molecular weight, the two earliest time increments are probably C_1 to C_4 hydrocarbons. It should be noted that fuel-rich combustion of ethylene is known to produce significant quantities of methane, acetylene, and selected unsaturated C_4 hydrocarbons, while C_3 and C_5 species are usually absent (Lam et al. 1990). Species which elude during the 4-6 minute increment probably do not adhere well to the microtrap and move swiftly through the column due to their small size (Mitra 1996), while the larger molecules which elude during the 7-9 minute interval are held by the microtrap, but only loosely. Once the trap is heated, these species are easily removed by the passing carrier gas. The 16-20 time increment contains at least C_6 species. Not only was benzene (retention time = 19.4 minutes) found to elude during this interval, but a strong, consistent peak at a retention time of 17 minutes was evident in both the C_1-C_6 standard and experiment. This peak may be a C_6 species, although no further study was done to confirm this.

Two additional observations can be drawn from the qualitative results. It is possible that the 11-13 increment from the GC standard is the C_5 hydrocarbon. Even during very fuel-rich combustion, it is unlikely that a significant amount of C_5's would be

produced (Lam et al. 1990). This explains the lack of experimental peak area within the 11-13 minute interval, especially when compared with the large peak area seen in Figure 6.9. Another general conclusion that can be made about the experimental integrated areas is that any significant peaks beyond 19.4 minutes are likely PICs which are larger than benzene. In the 20-30 minute time period, there is an incremental increase in area with the increase in equivalence ratio. The species which elude during this interval for the most part would exceed the molecular weight of benzene. Such species have also been observed during fuel-rich combustion (Lam et al. 1990).

Since none of the integrator peaks, other than benzene, are definitively identified, actual concentrations were not determined. The observations made during this section are speculative and warrant further investigation subsequent to the current research effort.

CHAPTER 7

CONCLUSIONS

This thesis has presented two sets of experimental and modeling results from the combustion of ethylene and air in a two stage turbulent flow reactor. The first portion of the research effort focused on the validation of the reactor as a PSR+PFR sequence using four different reaction mechanisms. The second part of this work centered on the fuel-rich combustion of ethylene and air, specifically with the application of a microtrap (Mitra et al. 1995) to concentrate the combustion sample. A number of general conclusions can be drawn from these efforts.

The rebuilt reactor does behave as a PSR+PFR sequence over the combustion conditions of interest, but the validation of the reactor depends partly on the goodness of the mechanism used. Since the most accurate mechanism had been applied previously to the same system and yielded excellent results (Mao 1995), its success in modeling the current results is not surprising.

For all runs, it was observed that an increase in the fuel equivalence ratio resulted in an increase in the carbon monoxide and light hydrocarbon concentrations. For the fuel-rich effort, the same trend was seen for the higher molecular weight species. Attempts to model these concentrations with the Zhong mechanism (Zhong et al. 1996) yielded mixed results perhaps because the aromatic mechanism was built on a weak C_1/C_2 hydrocarbon base as evidenced by its weak performance in modeling these species.

The microtrap demonstrated great potential as an on-line technique to concentrate low levels of PICs from combustion gases. However its utility, as currently configured,

is hindered in the presence of the larger hydrocarbon concentrations which exist under elevated equivalence ratios. Modification in the sample collection protocol and/or GC analysis are needed to fully exploit the potential of the on-line microtrap in combustion applications.

Although all experimental efforts were focused on ethylene combustion, additional laboratory work was done to assist future efforts. An atomizer/vaporizer unit was made and successfully tested using methylene chloride as the liquid dopant. Specific operating instructions are included in Appendix B. Although the ethylene database compiled during this research will be a significant asset to the collaborative effort between NJIT and MIT, this new apparatus will further enhance the overall goal to attain a better understanding of PIC formation and emission.

APPENDIX A

FIGURES

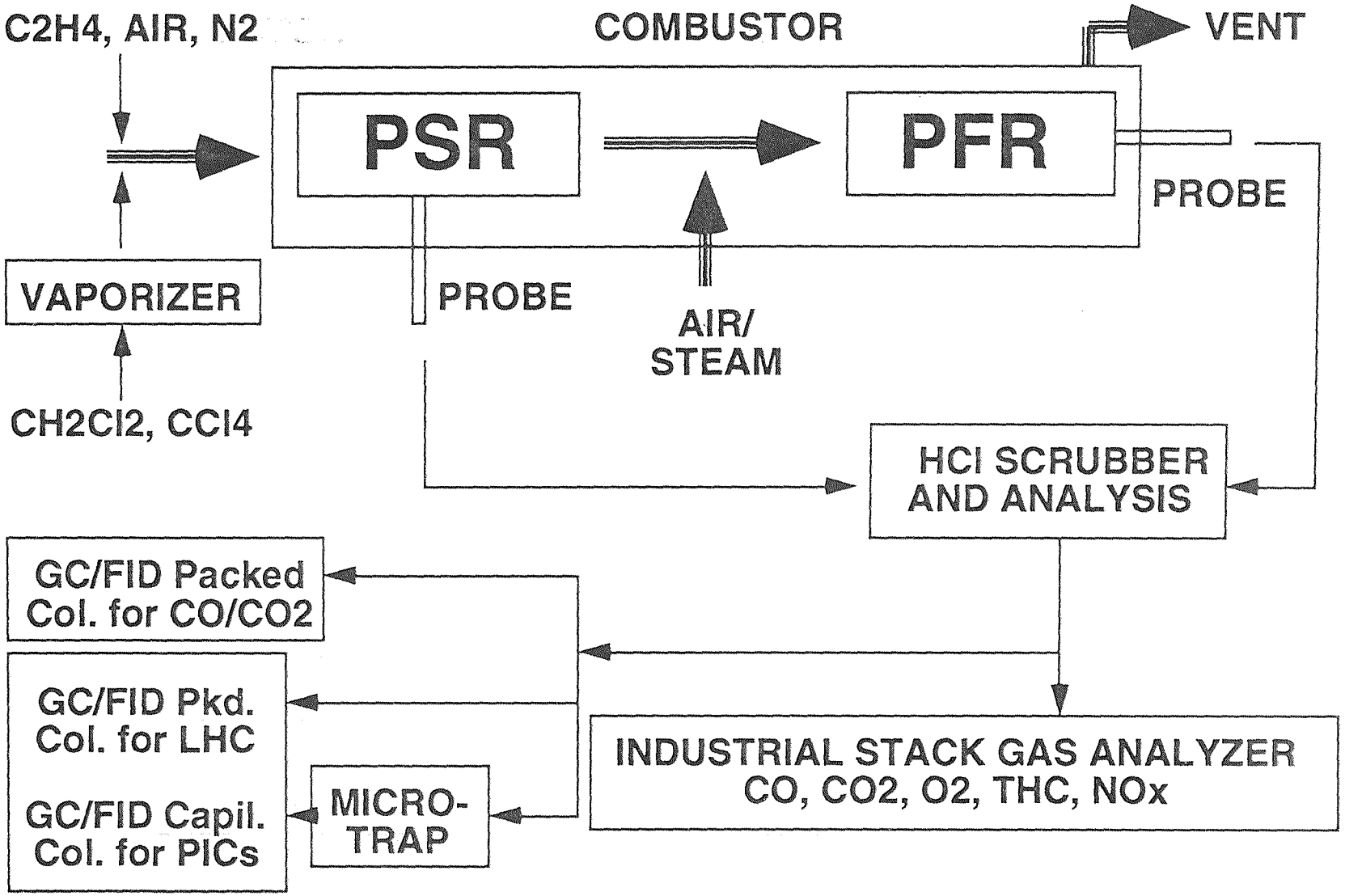

Figure 3.1 - Overall Schematic of Two-Stage Turbulent Flow Reactor Facility

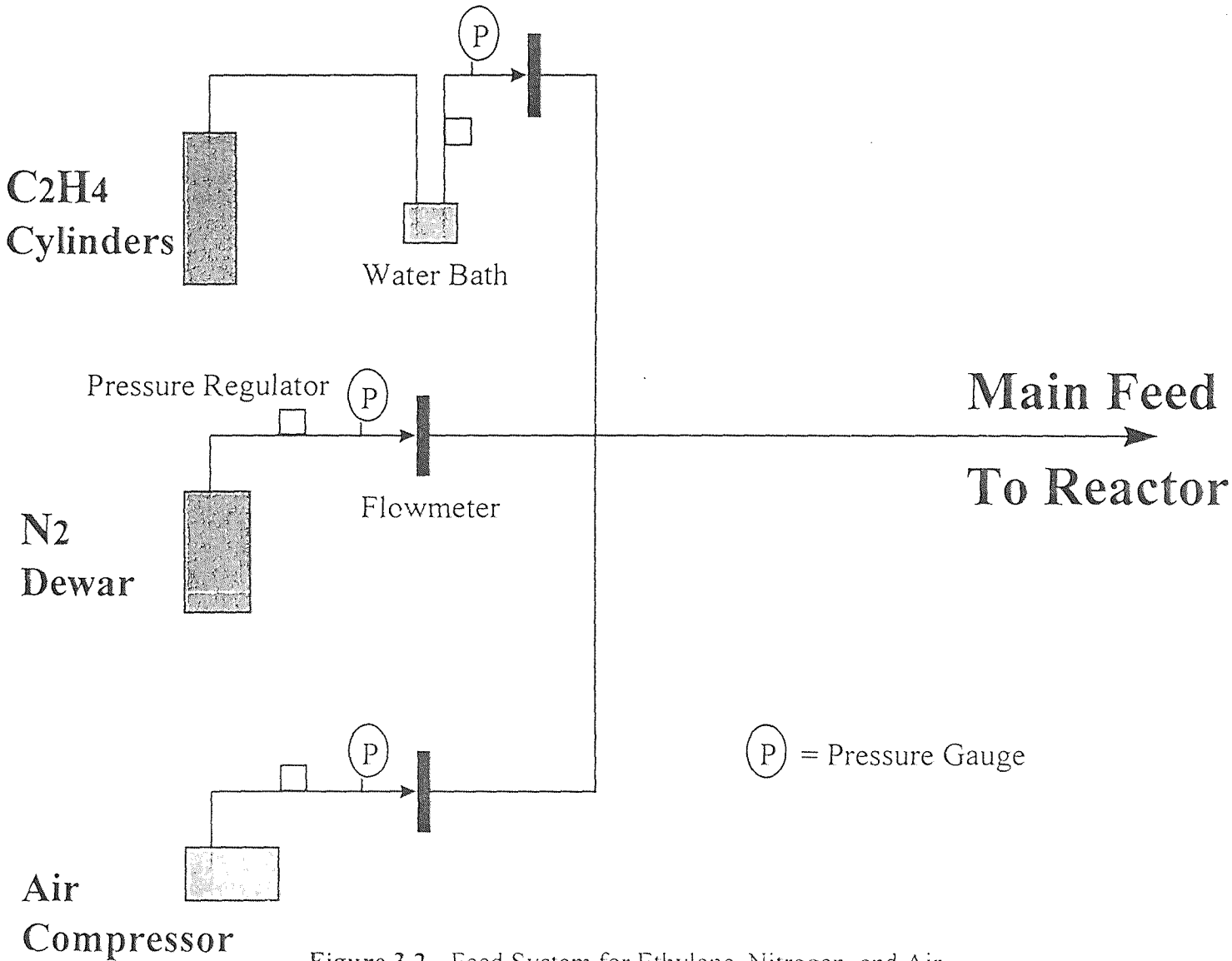

Figure 3.2 - Feed System for Ethylene, Nitrogen, and Air

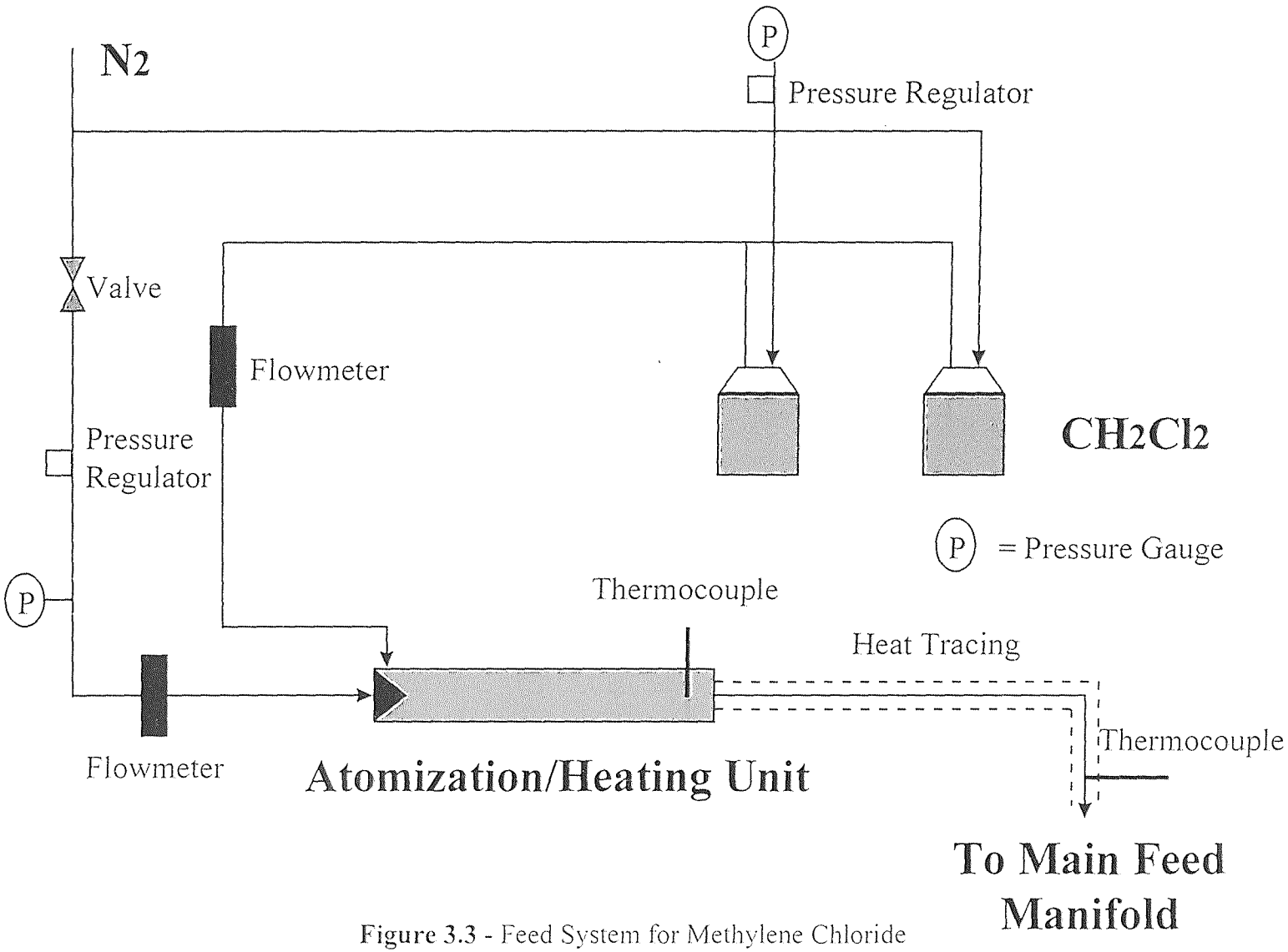

Figure 3.3 - Feed System for Methylene Chloride

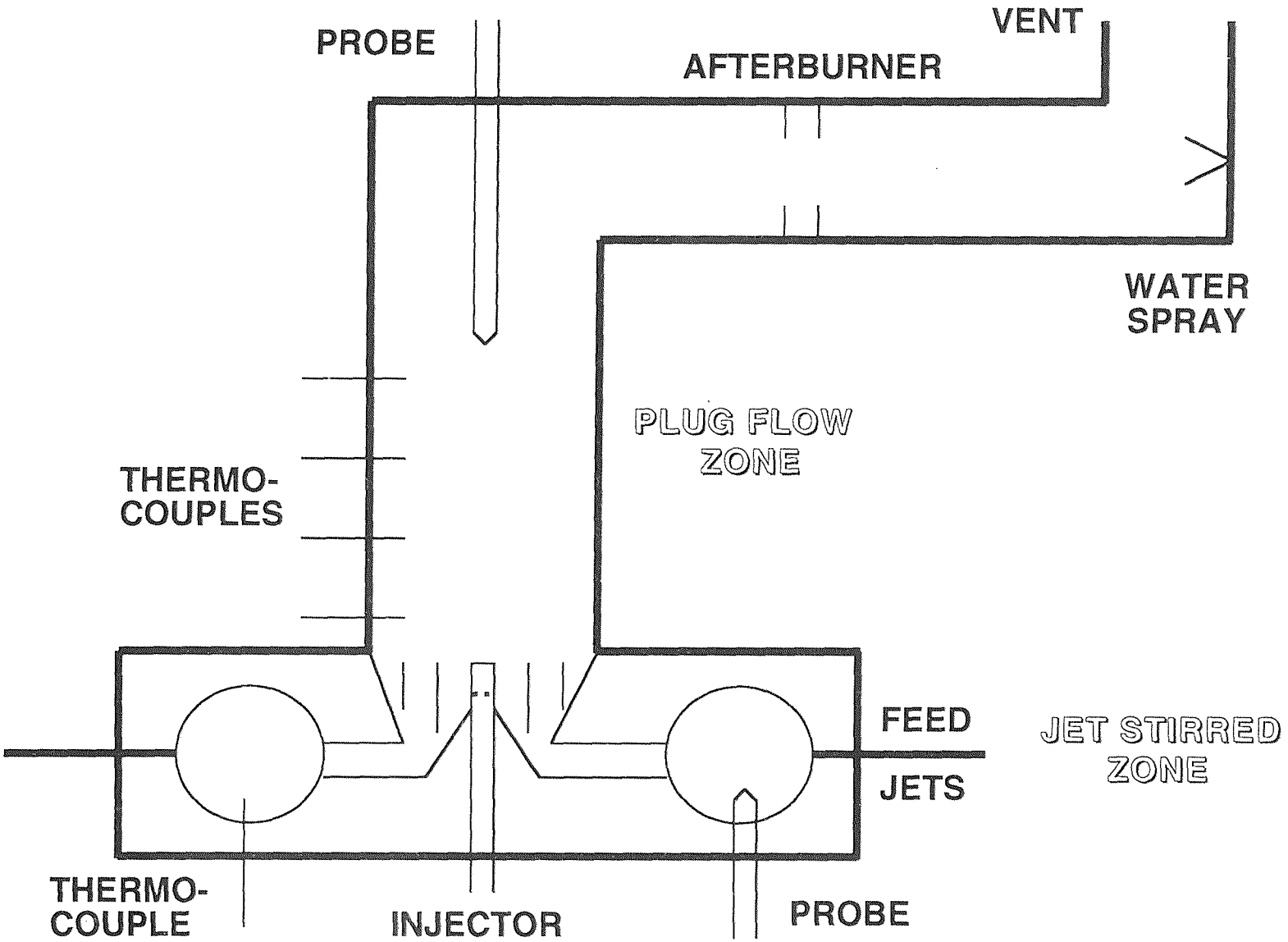

Figure 3.4 - Two-Stage Turbulent Flow Reactor

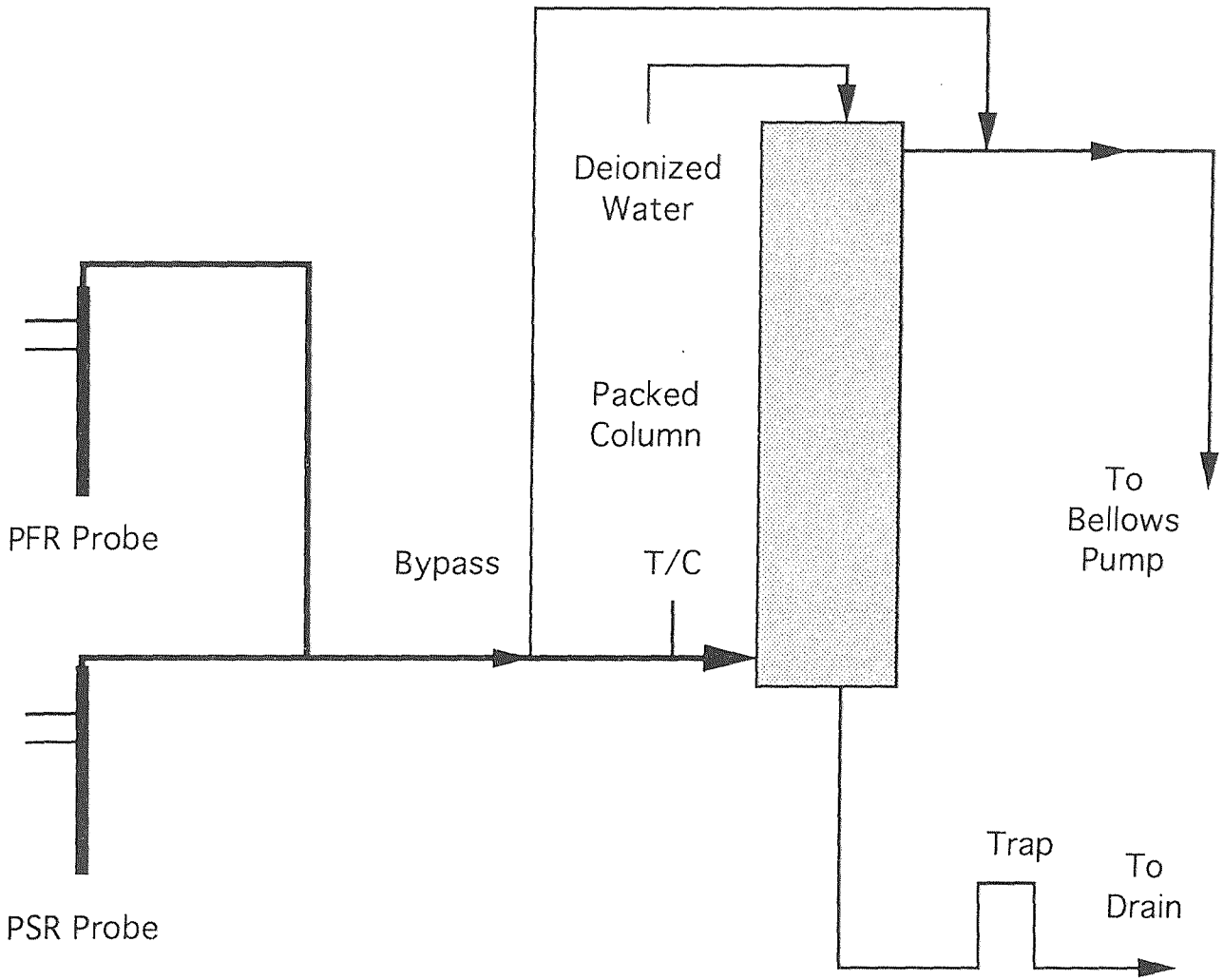

Figure 3.5 - Sampling System

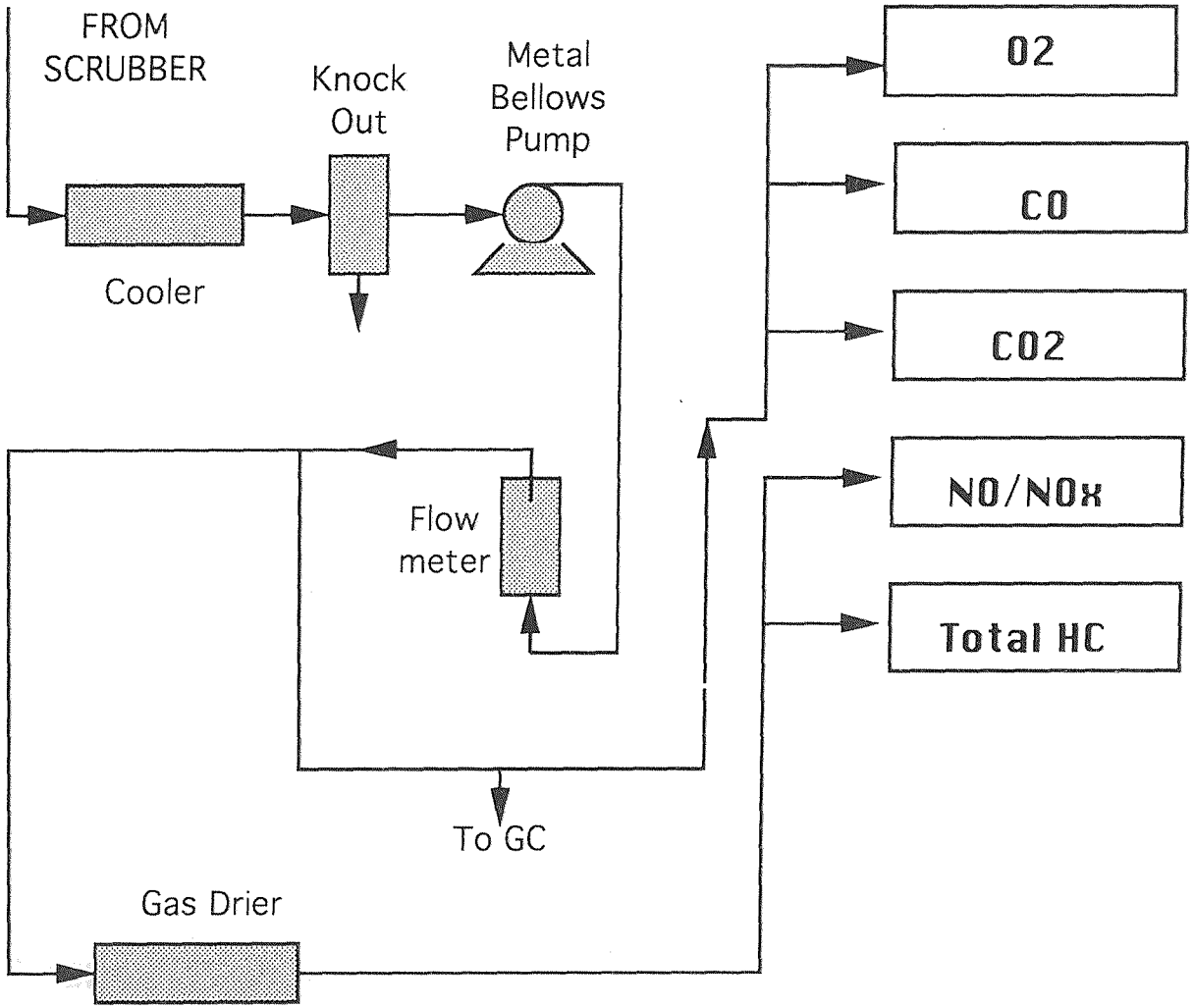

Figure 3.6 - Analytical System - Continuous Emission Monitors

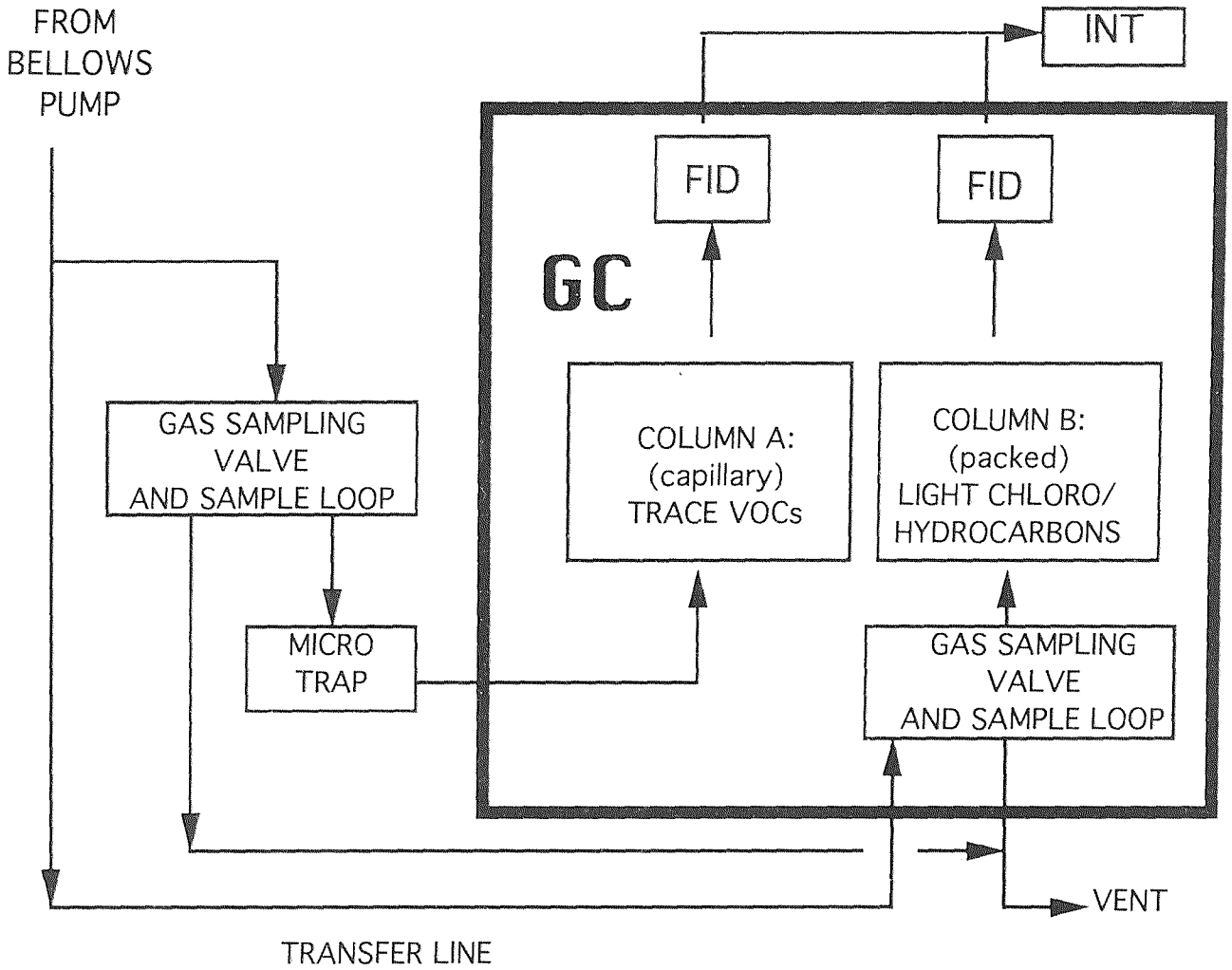

Figure 3.7 - Analytical System - Hewlett-Packard Gas Chromatograph

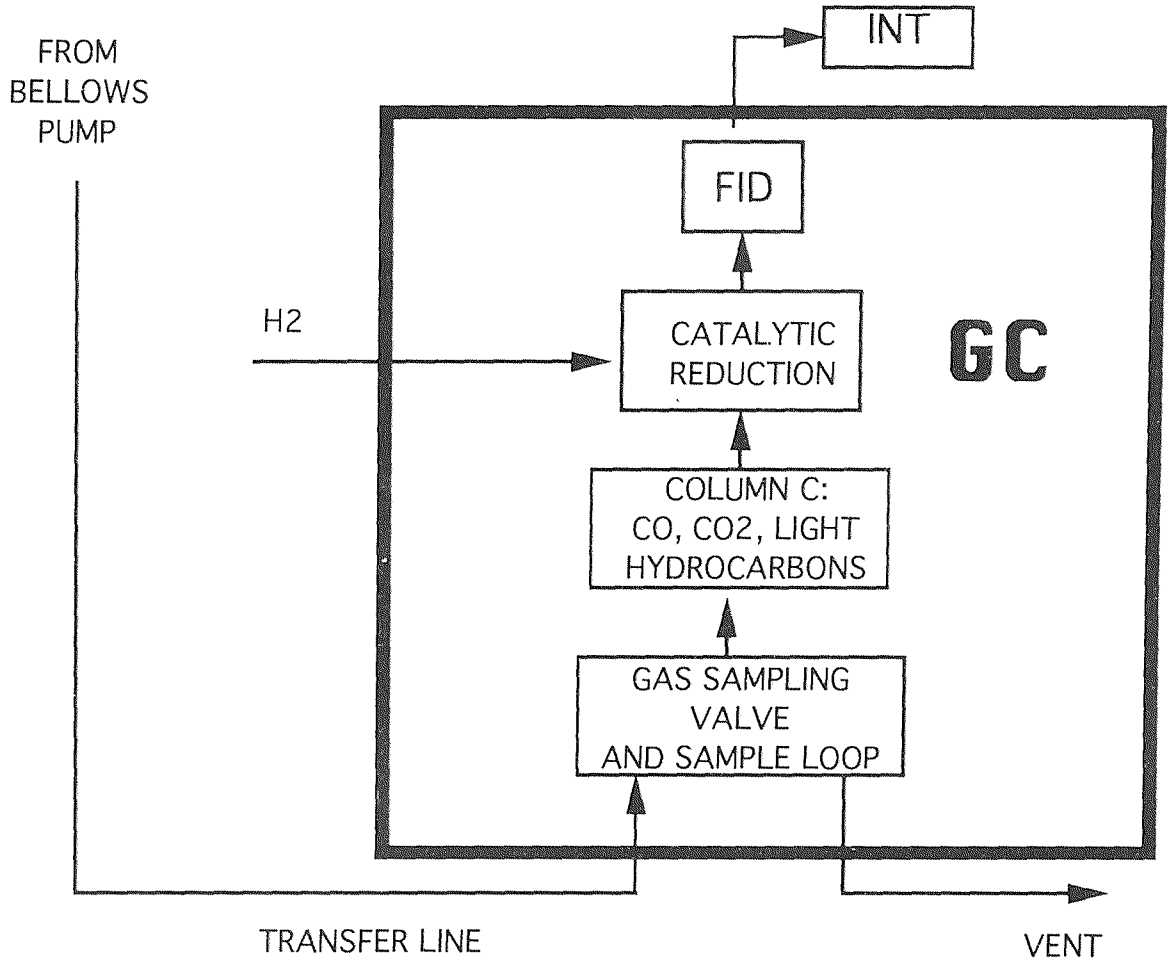

Figure 3.8 - Analytical System - Varian Gas Chromatograph

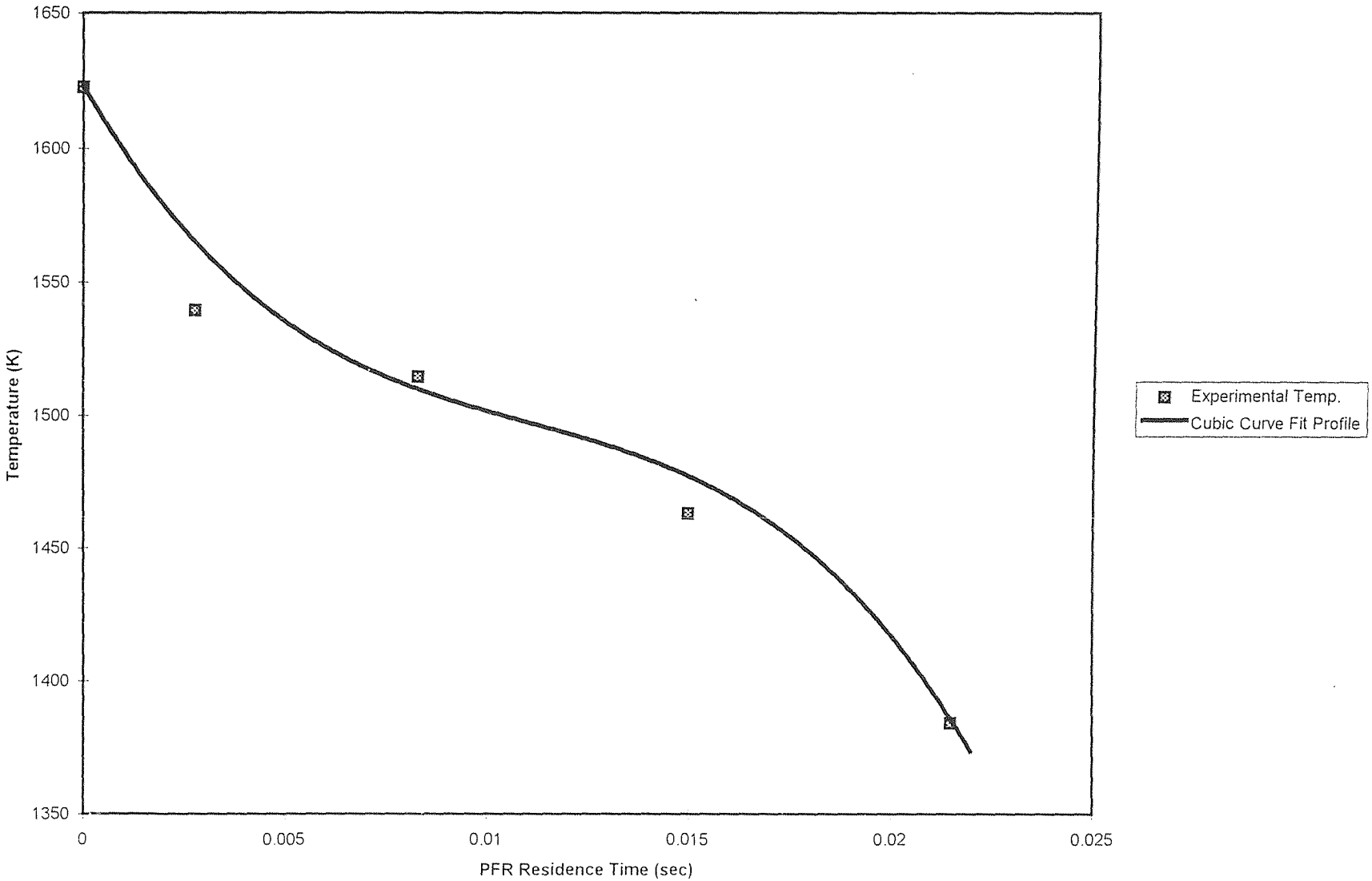

Figure 4.1 - Typical Temperature Profile in PFR

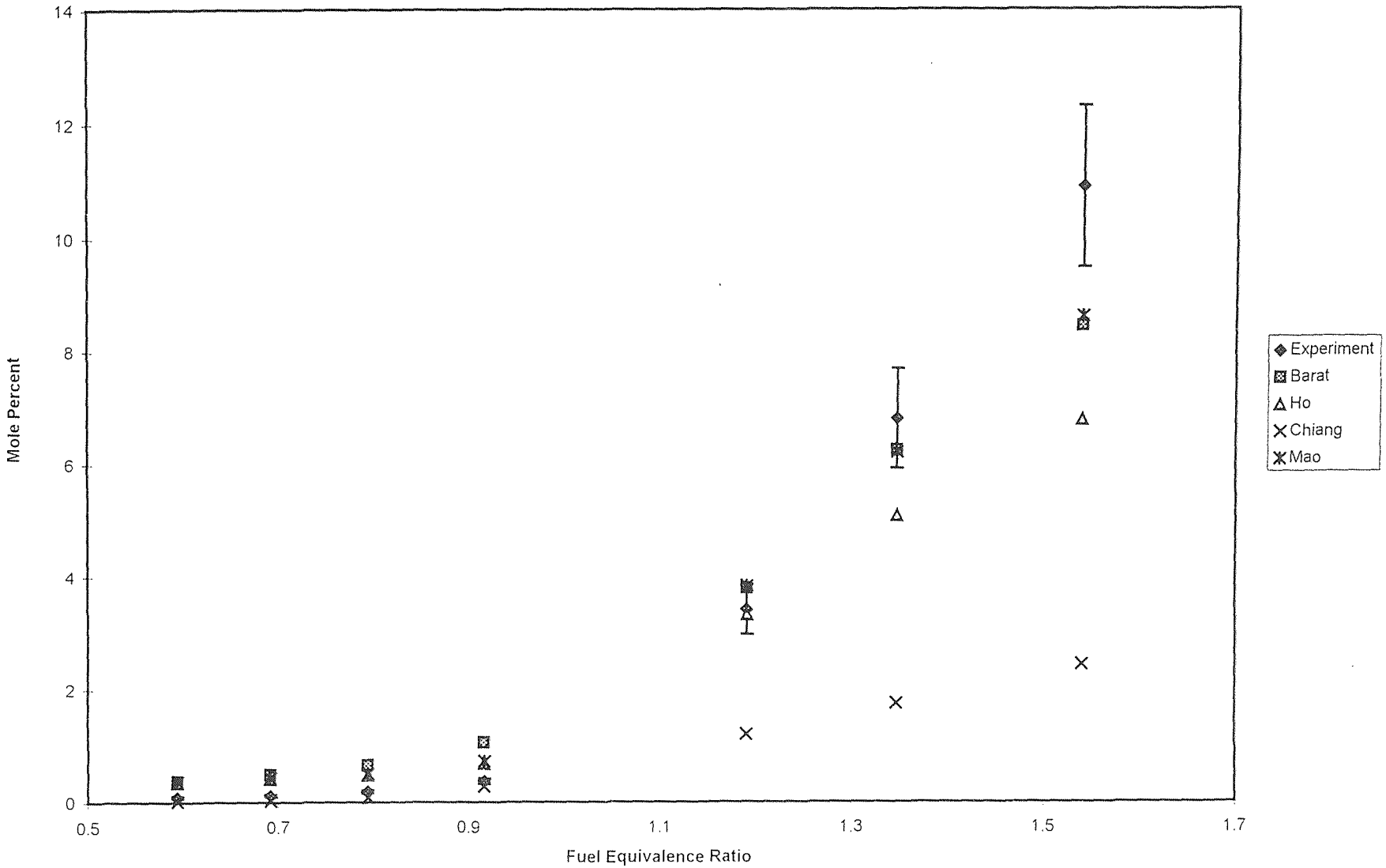

Figure 5.1 - CO Levels in First Stage

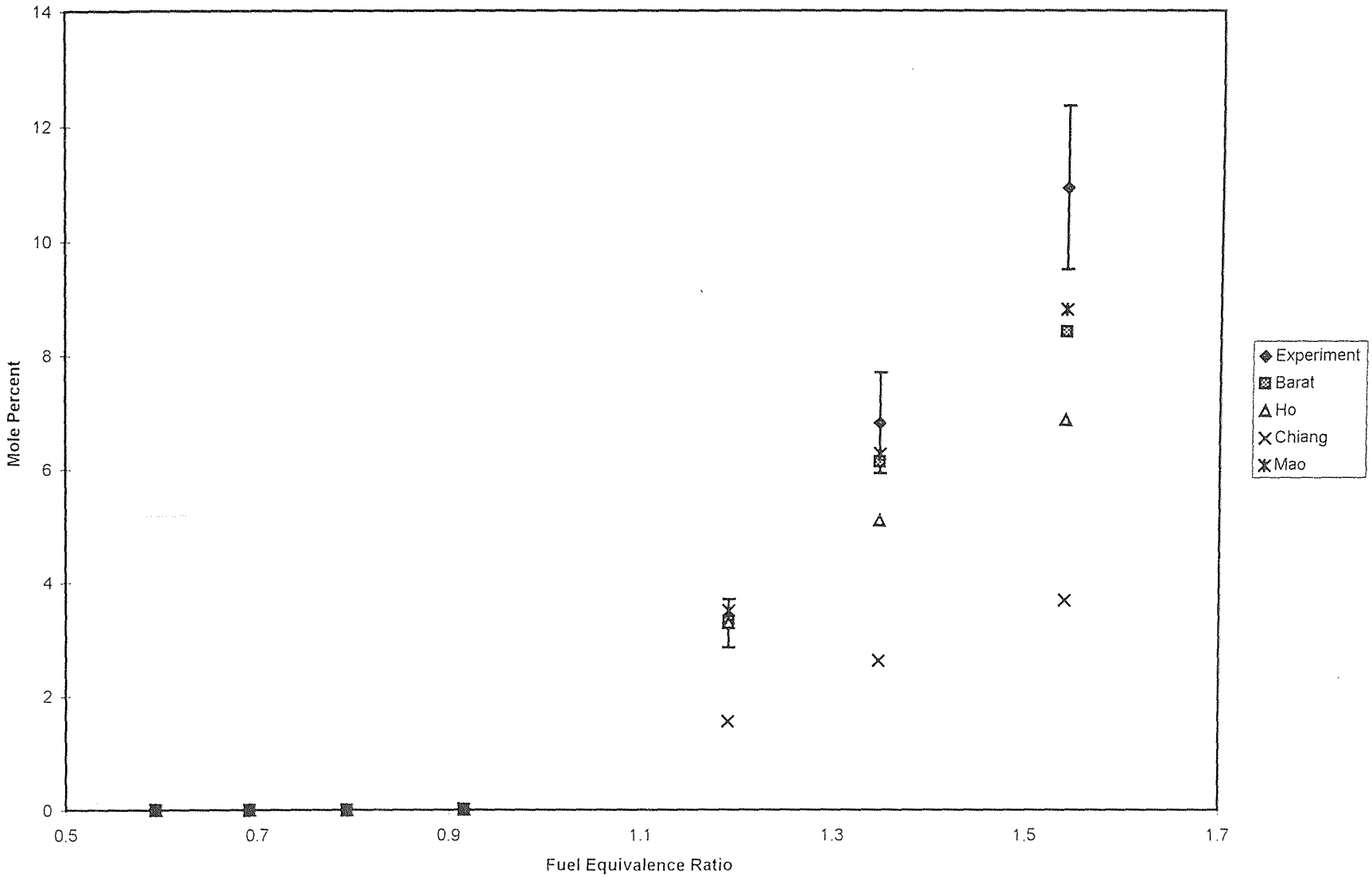

Figure 5.2 - CO Levels at Second Stage Outlet

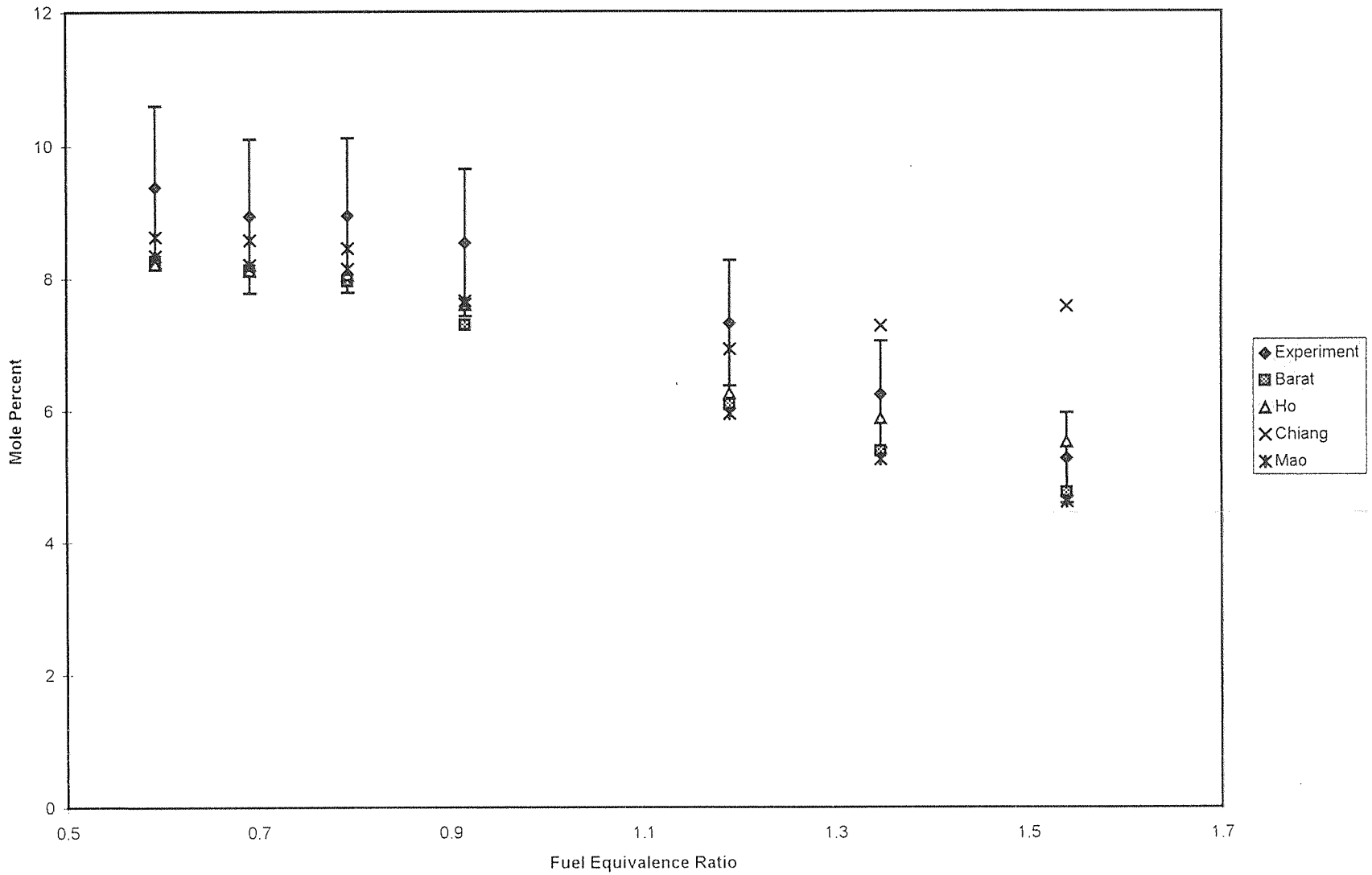

Figure 5.3 - CO_2 Levels in First Stage

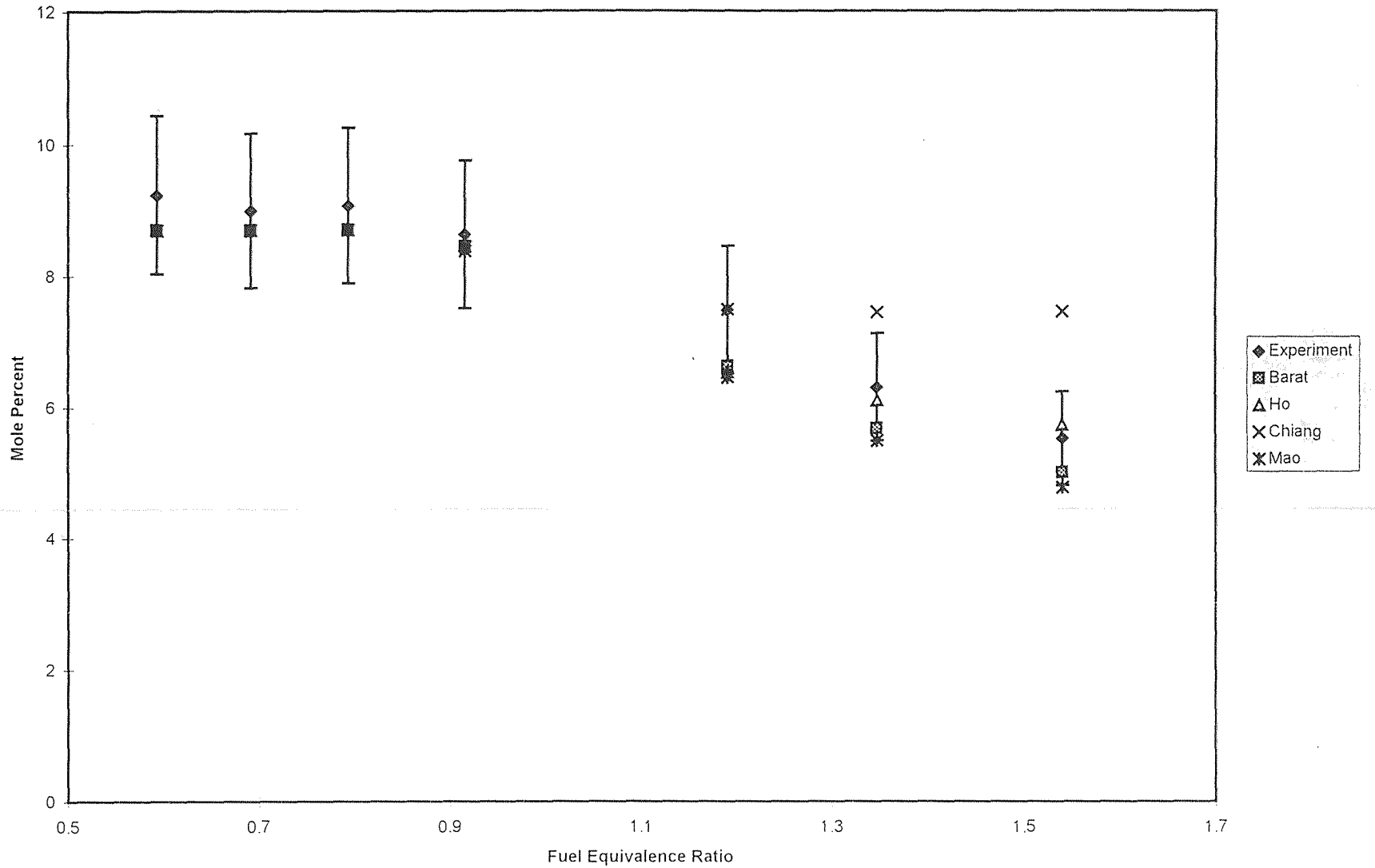

Figure 5.4 - CO_2 Levels at Second Stage Outlet

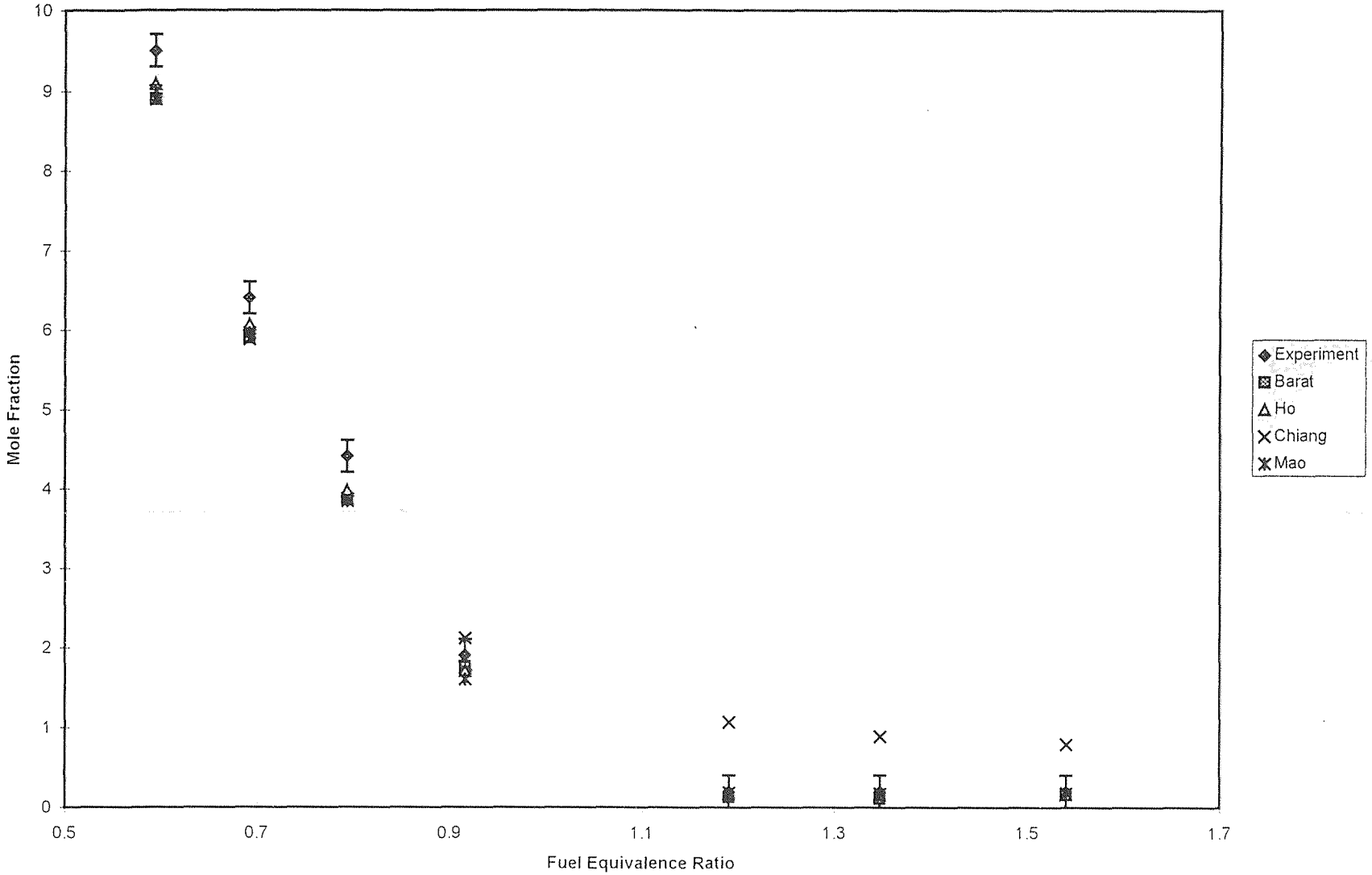

Figure 5.5 - O_2 Levels in First Stage

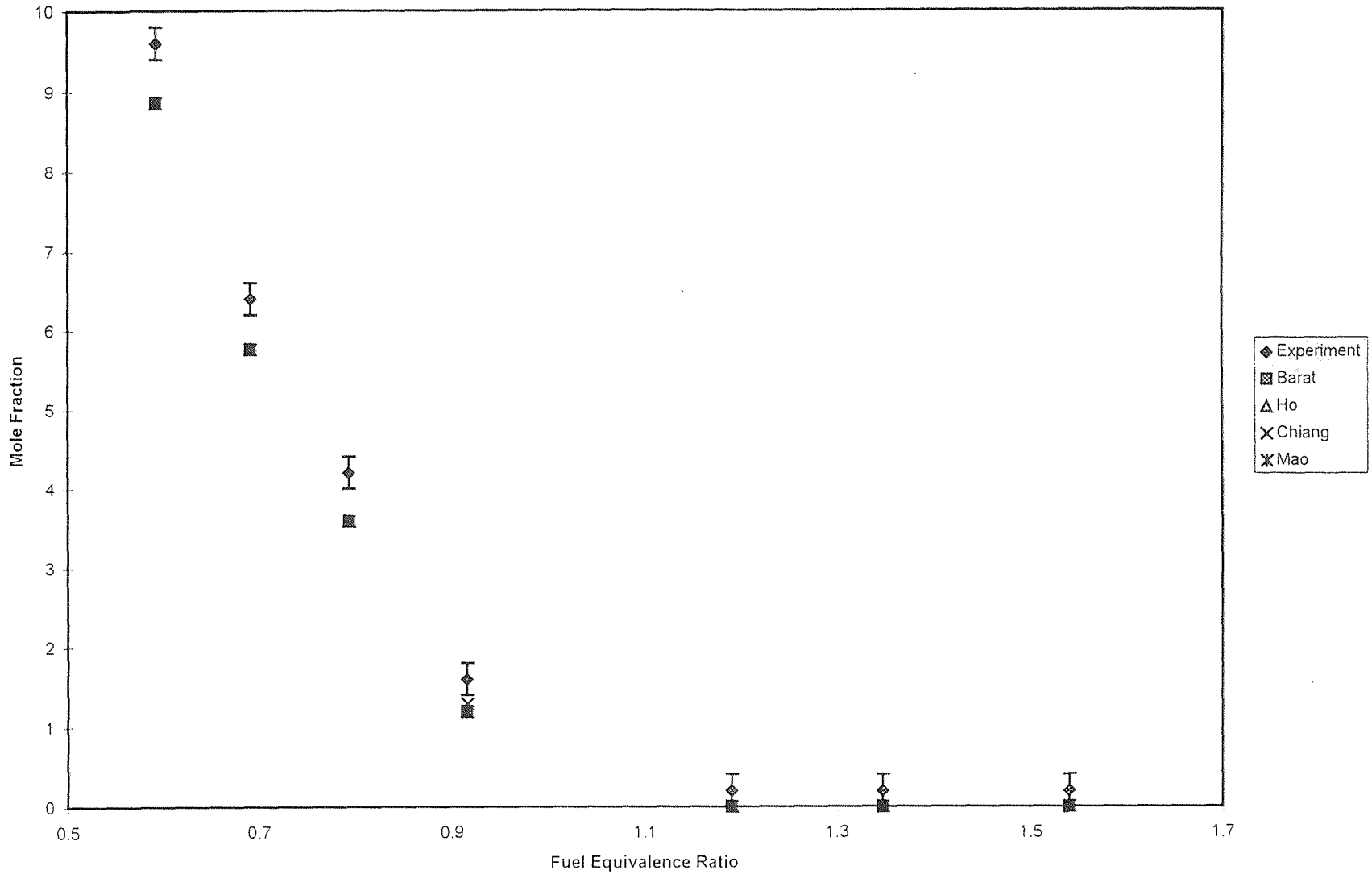

Figure 5.6 - O_2 Levels at Second Stage Outlet

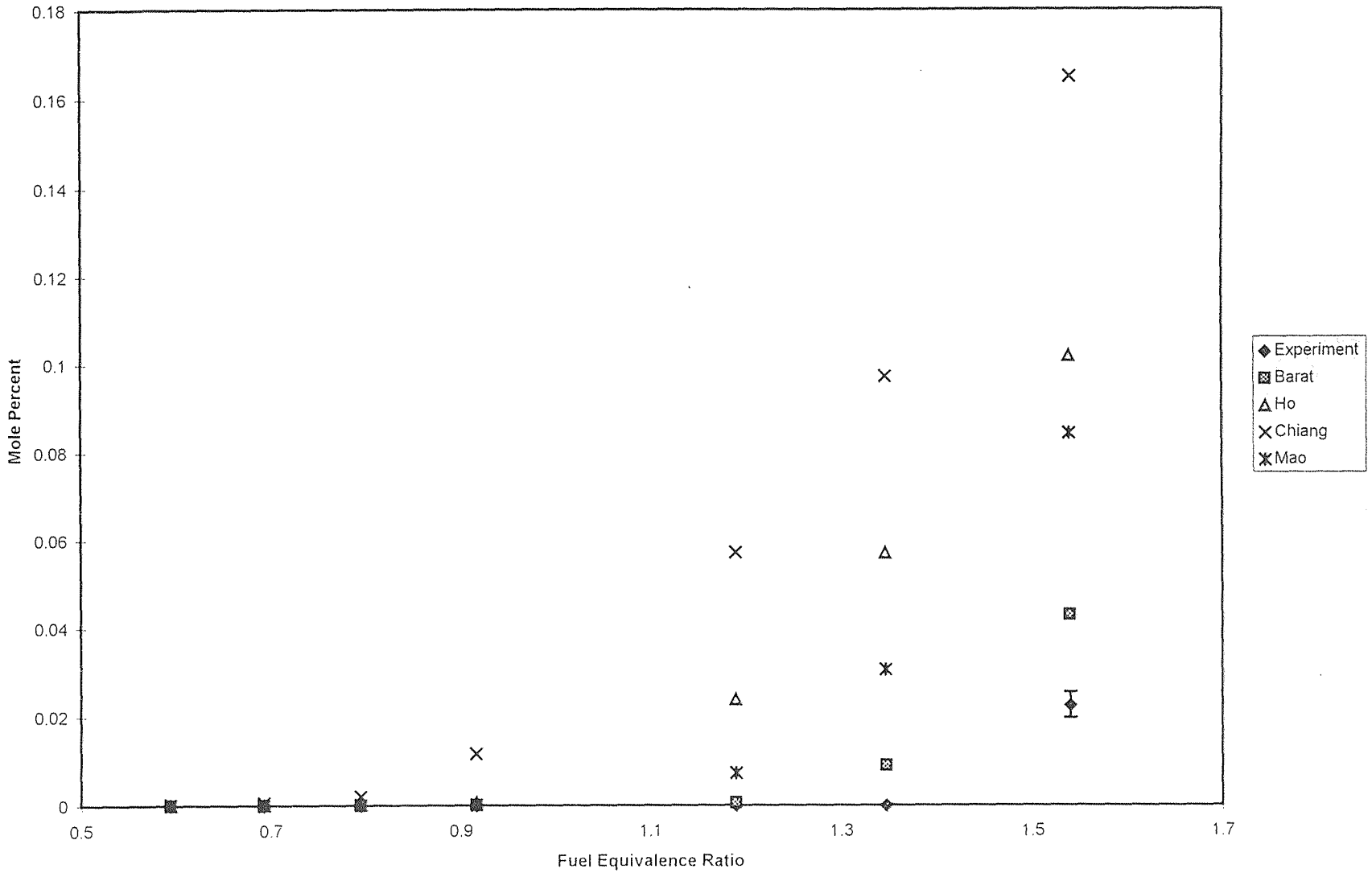

Figure 5.7 - CH_4 Levels in First Stage

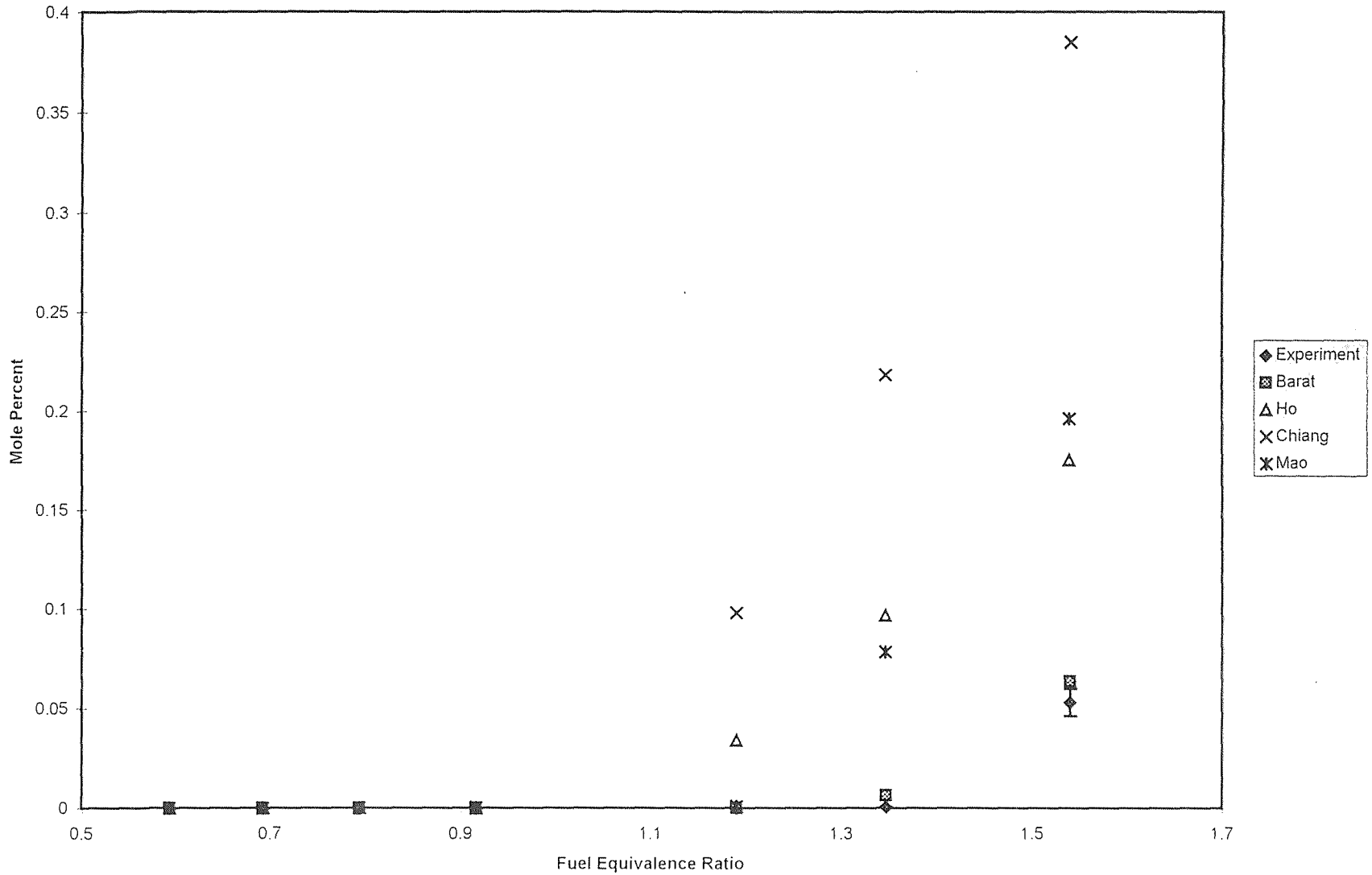

Figure 5.8 - CH_4 Levels at Second Stage Outlet

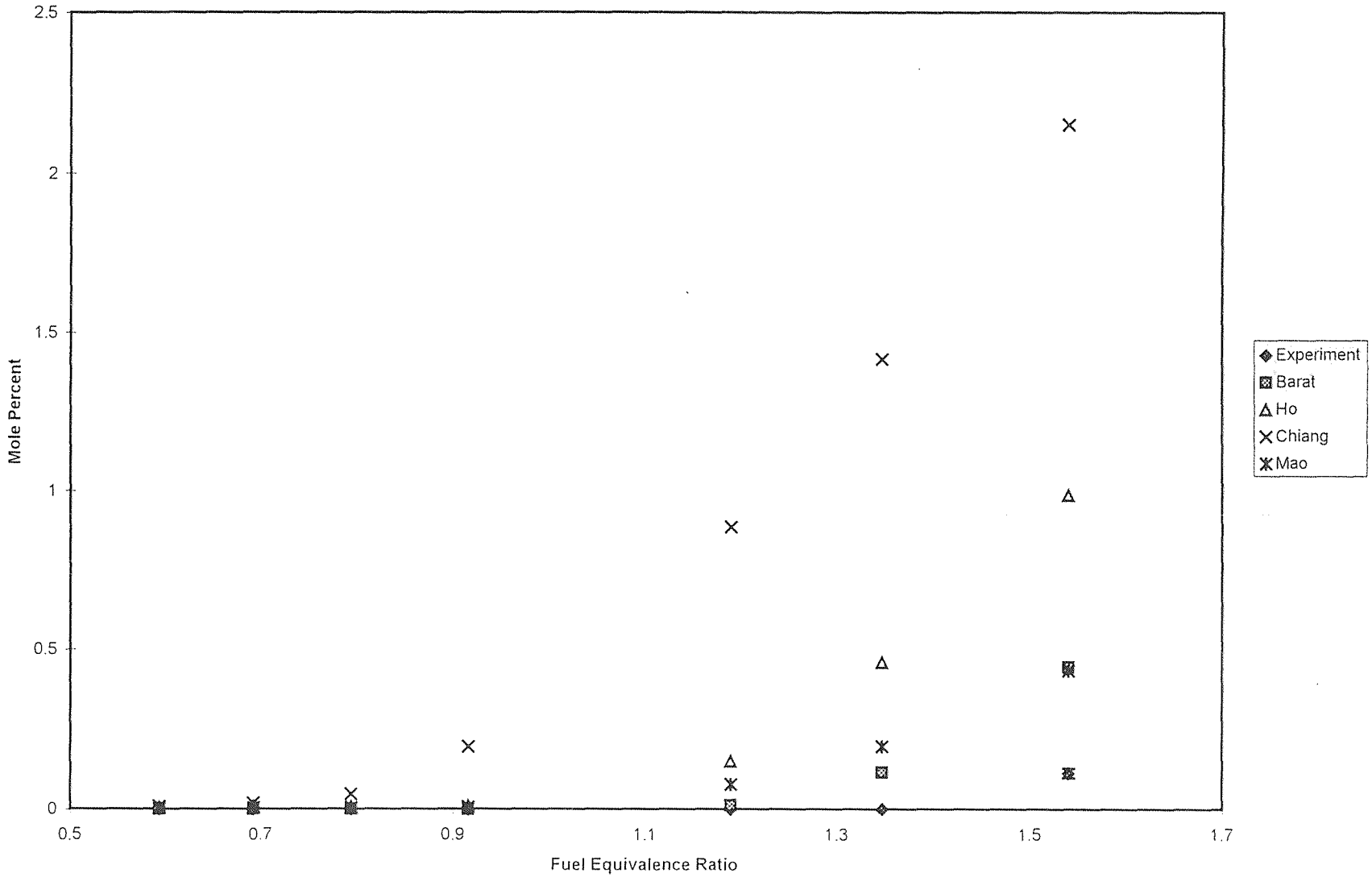

Figure 5.9 - C_2H_2 Levels in First Stage

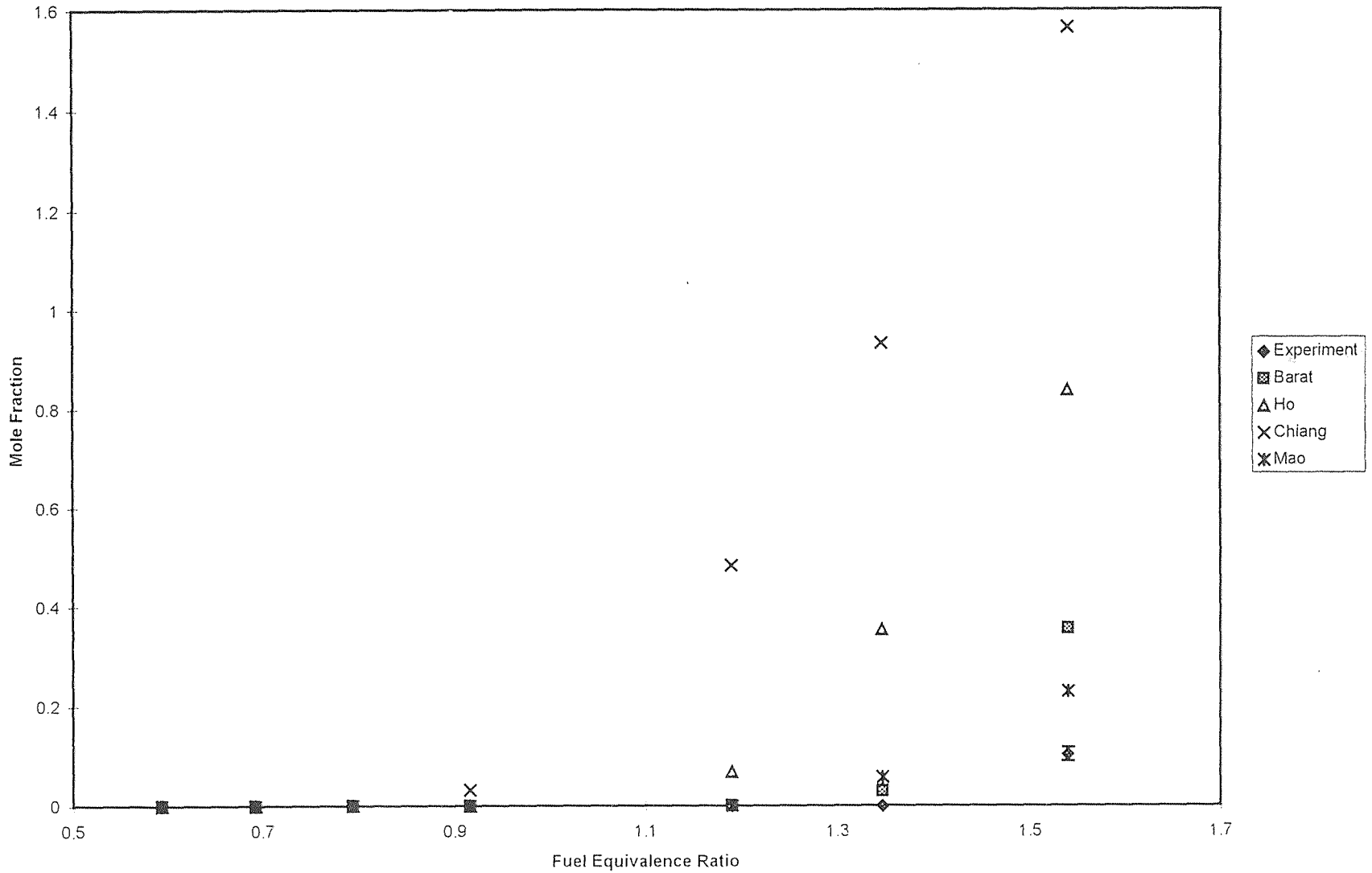

Figure 5.10 - C_2H_2 Levels at Second Stage Outlet

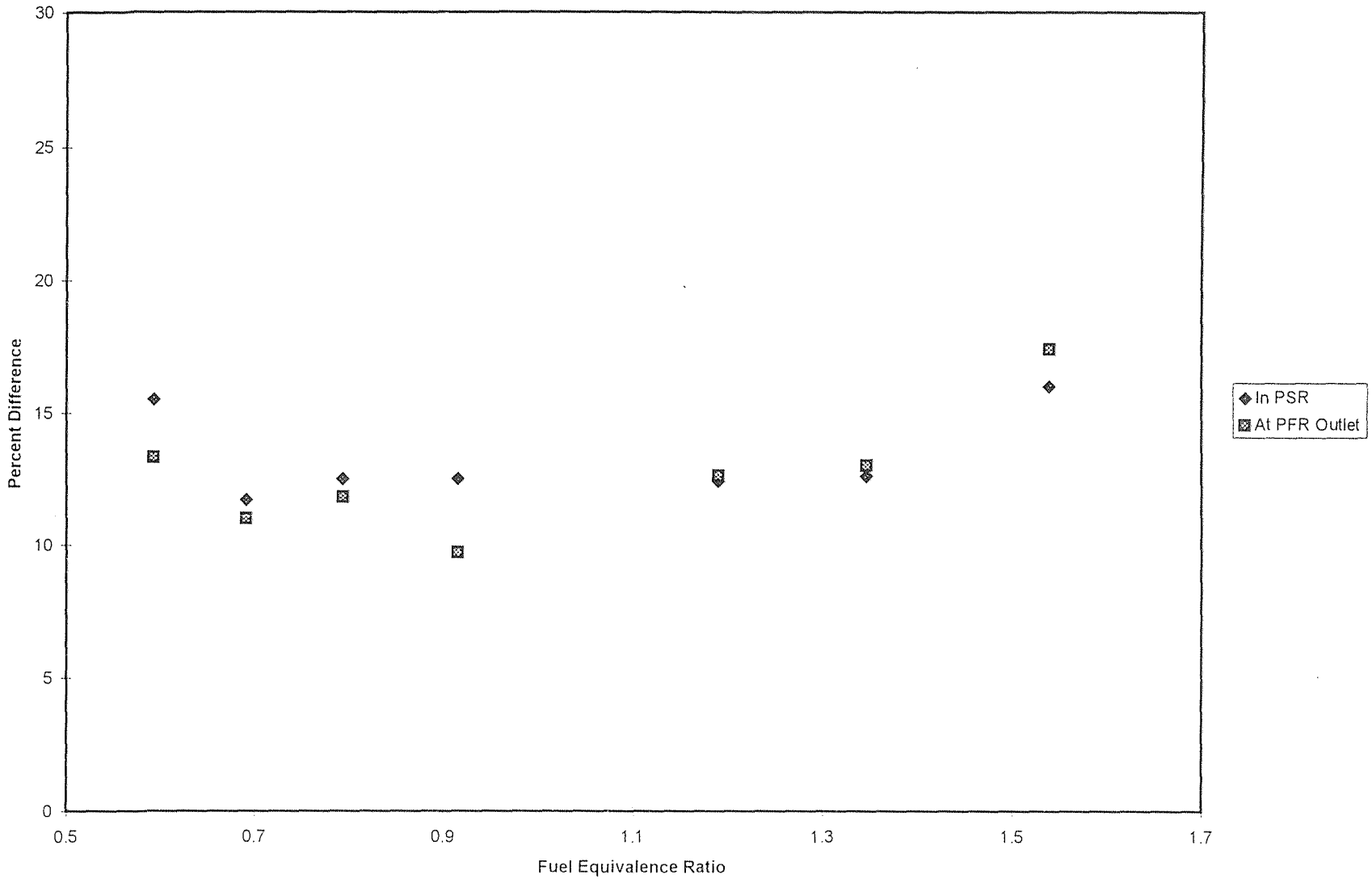

Figure 5.11 - Carbon Balance (Inlet vs. Outlet)

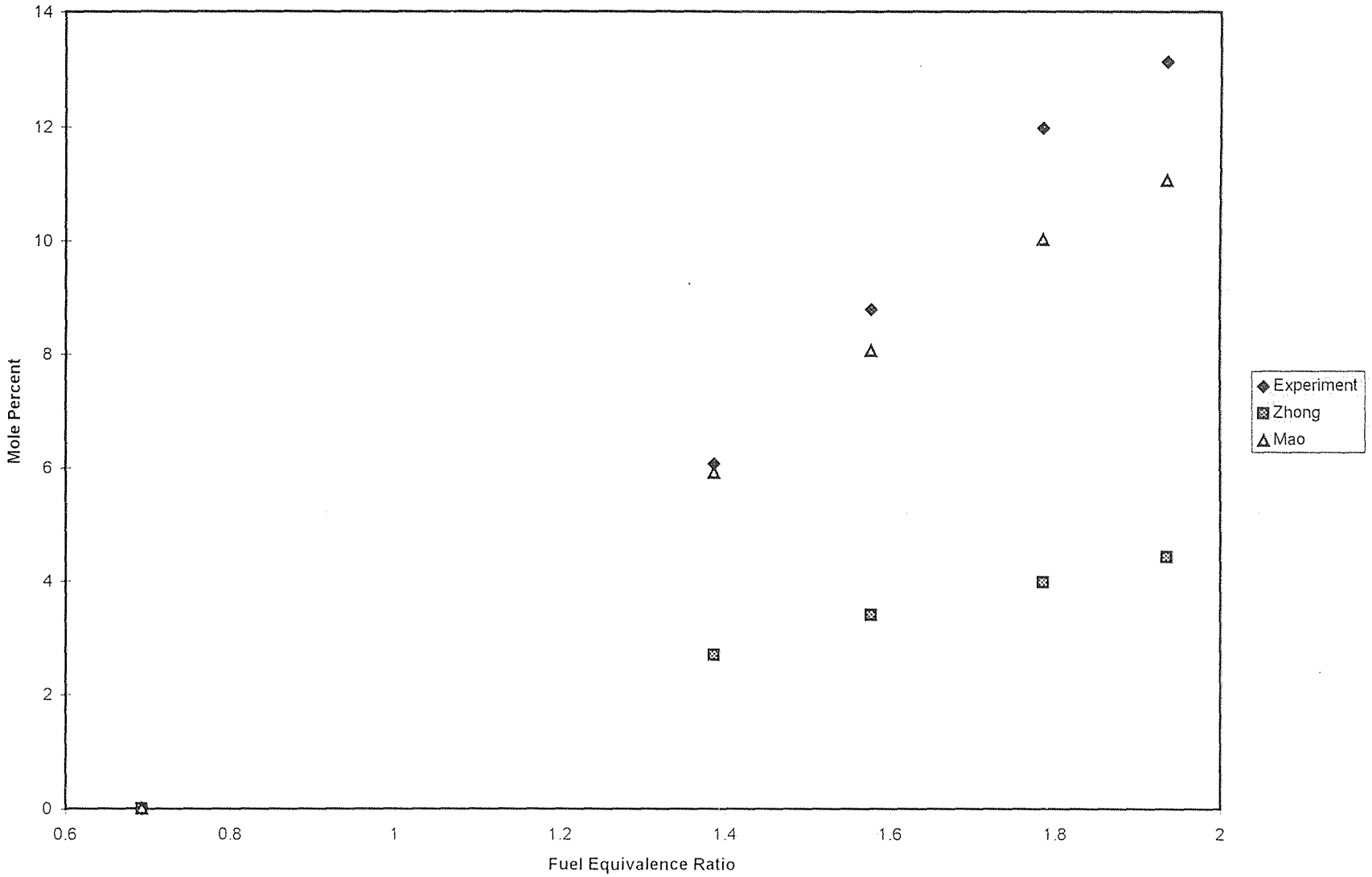

Figure 6.1 - CO Levels at Second Stage Outlet

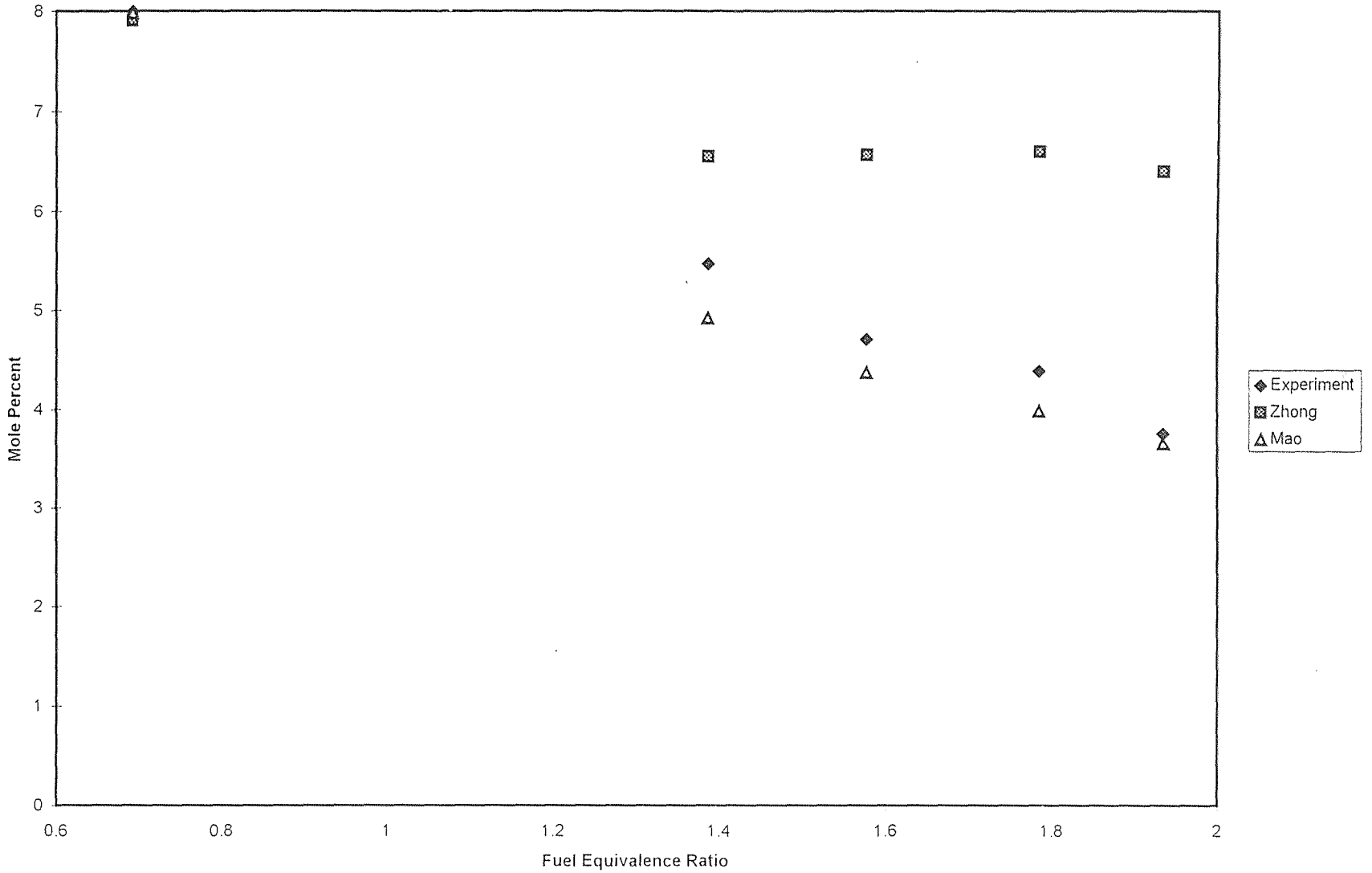

Figure 6.2 - CO_2 Levels at Second Stage Outlet

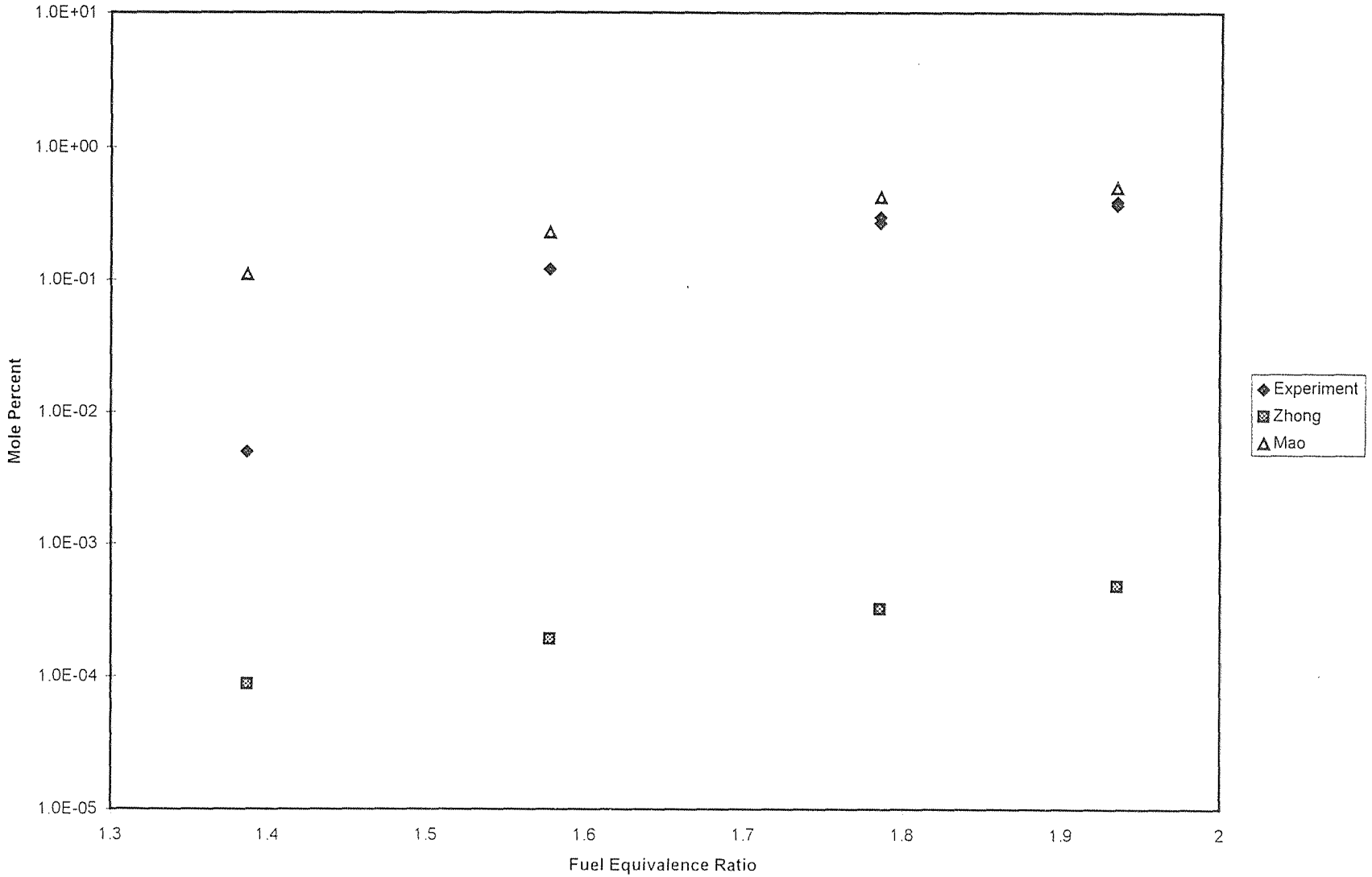

Figure 6.3 - CH_4 Levels at Second Stage Outlet

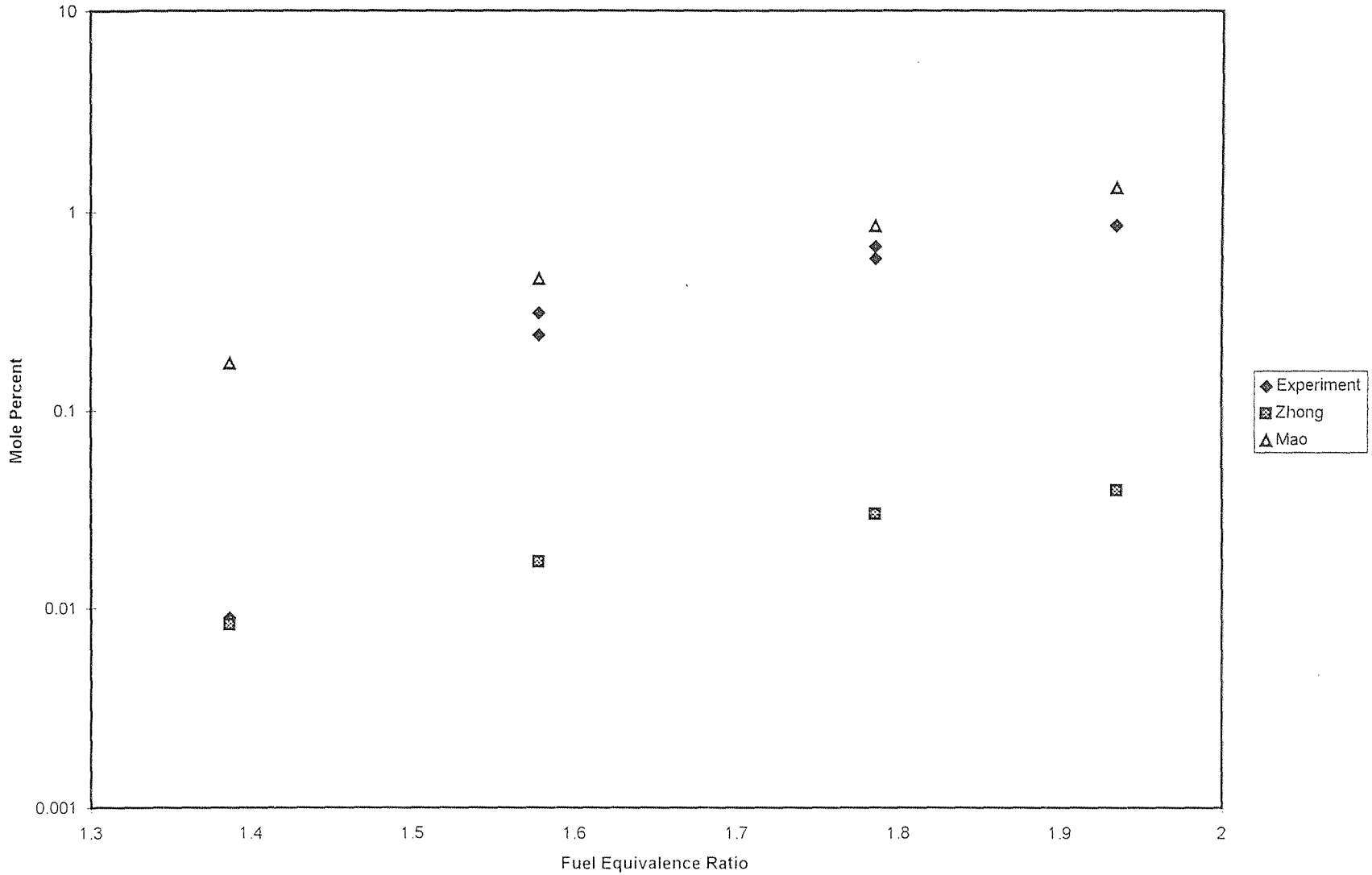

Figure 6.4 - C_2H_2 Levels at Second Stage Outlet

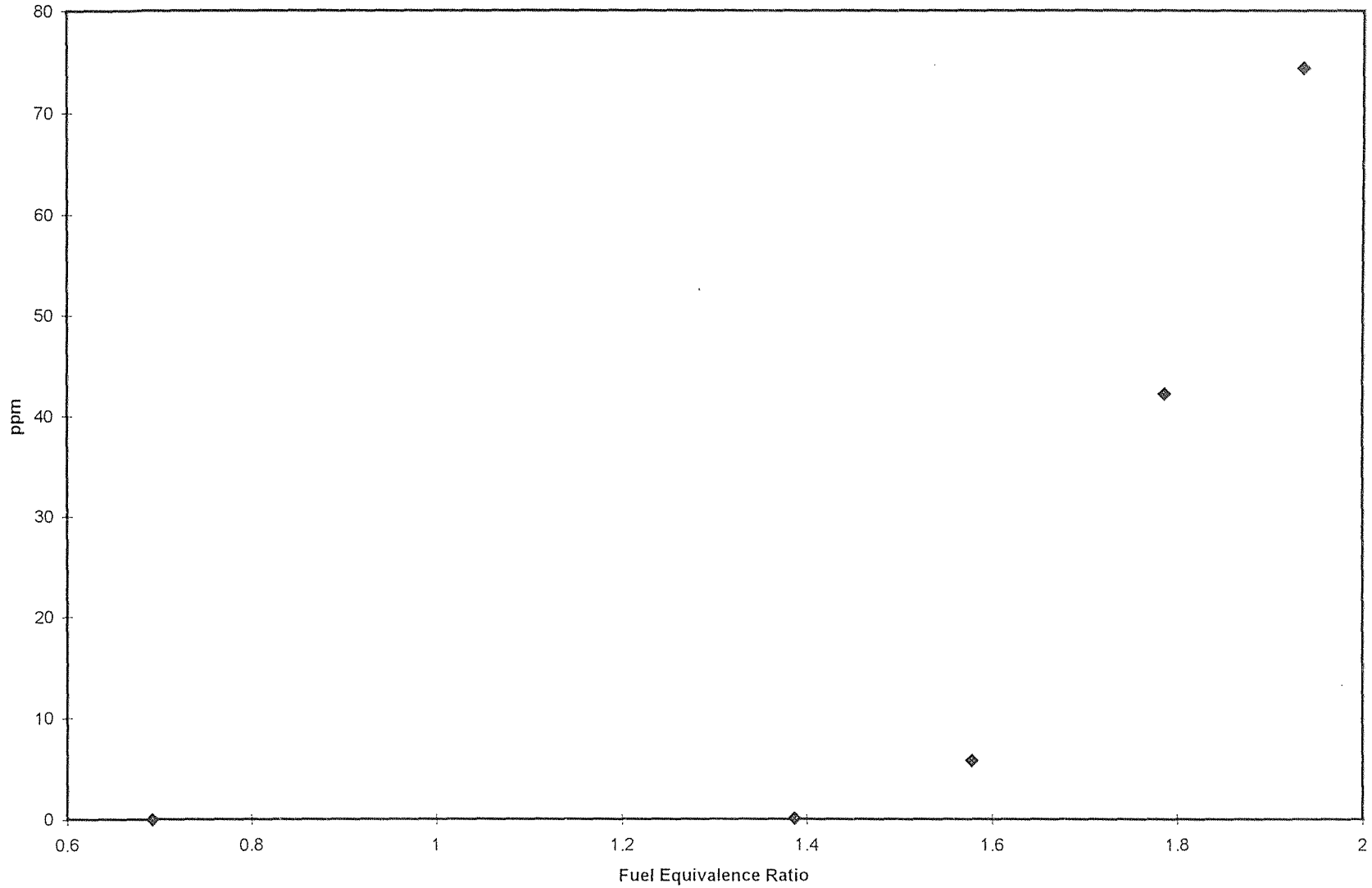

Figure 6.5 - Experimental C_6H_6 Levels at Second Stage Outlet

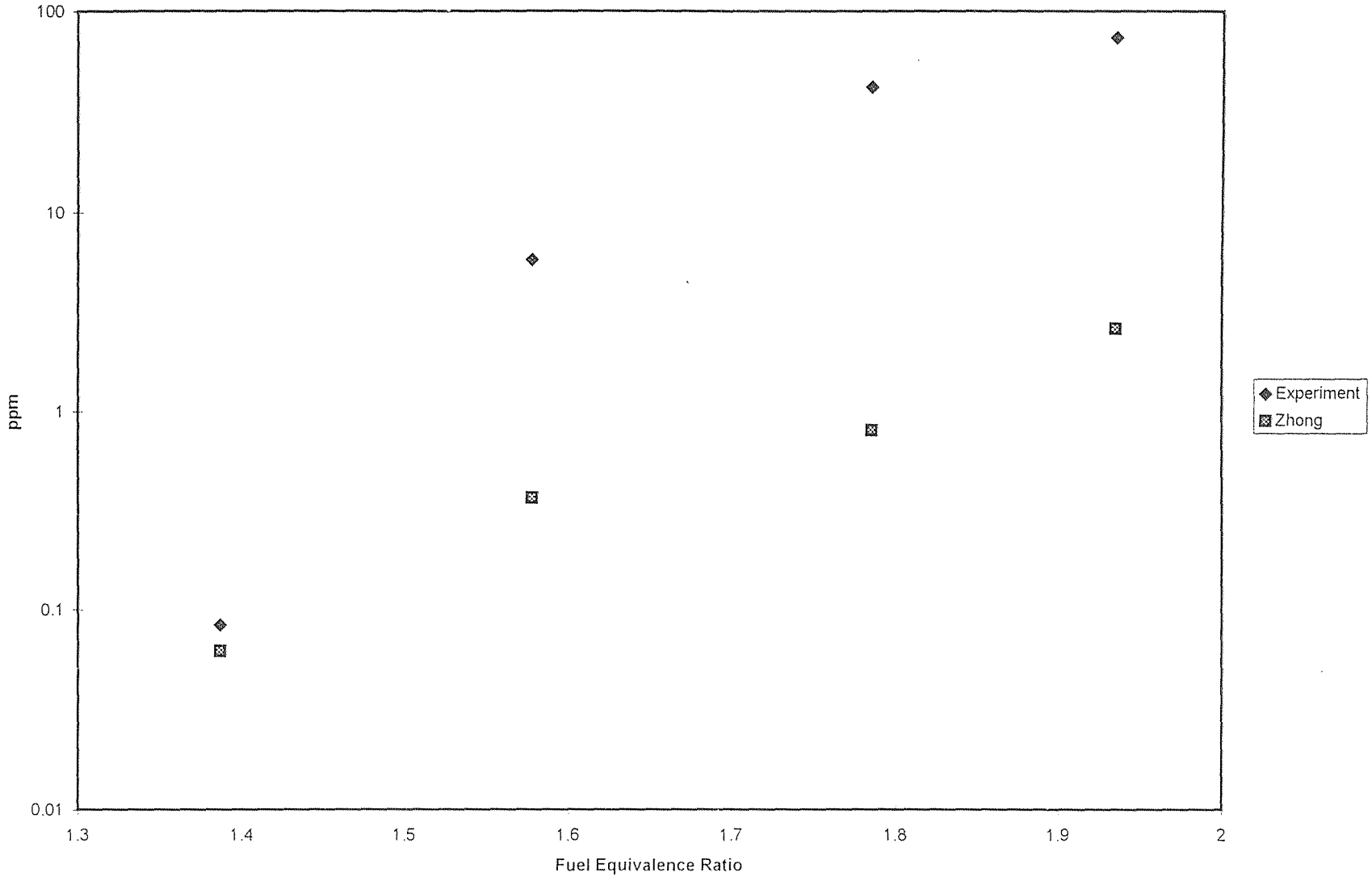

Figure 6.6 - C_6H_6 Levels at Second Stage Outlet

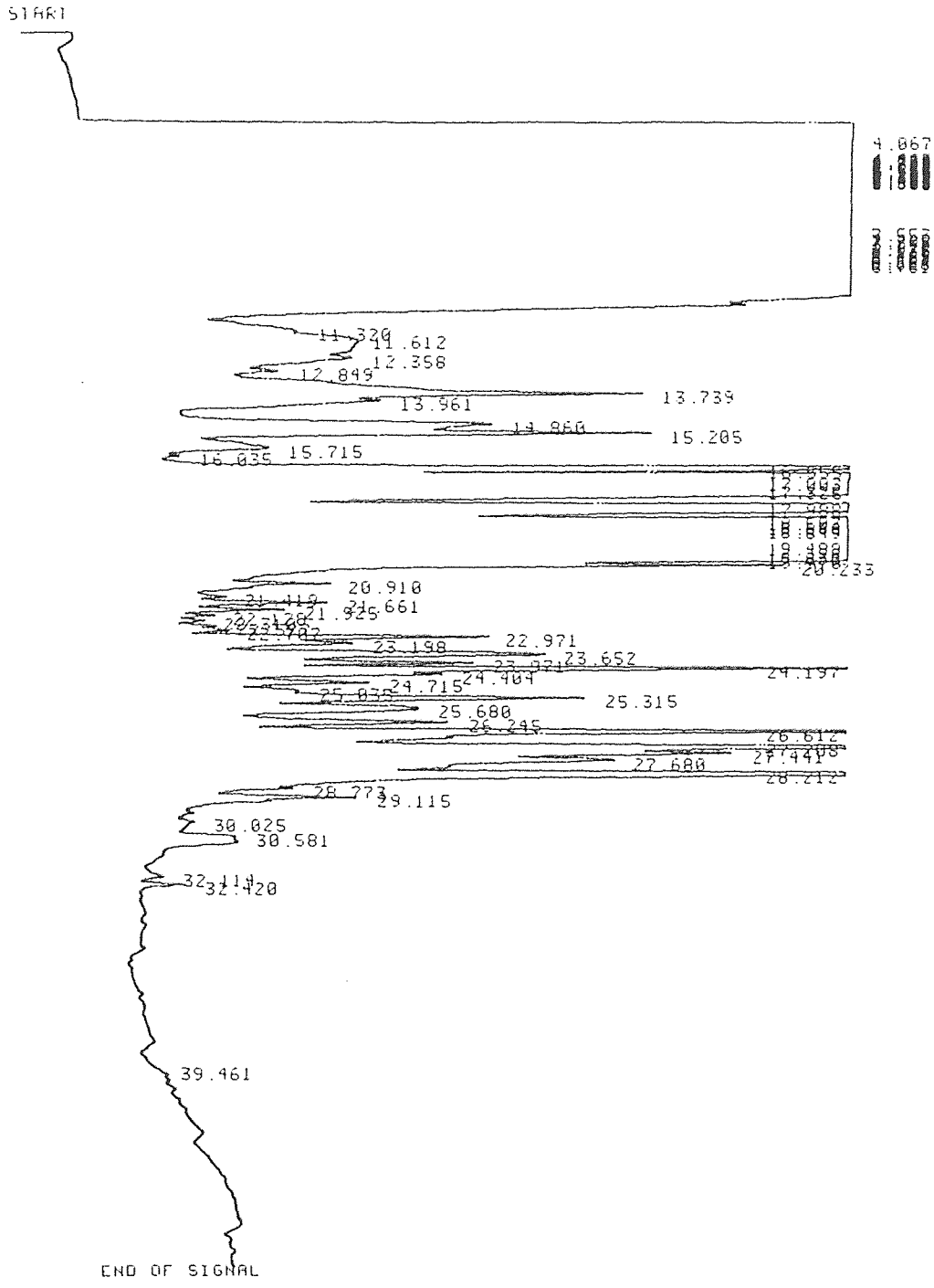

Figure 6.7 - Typical Experimental Chromatogram

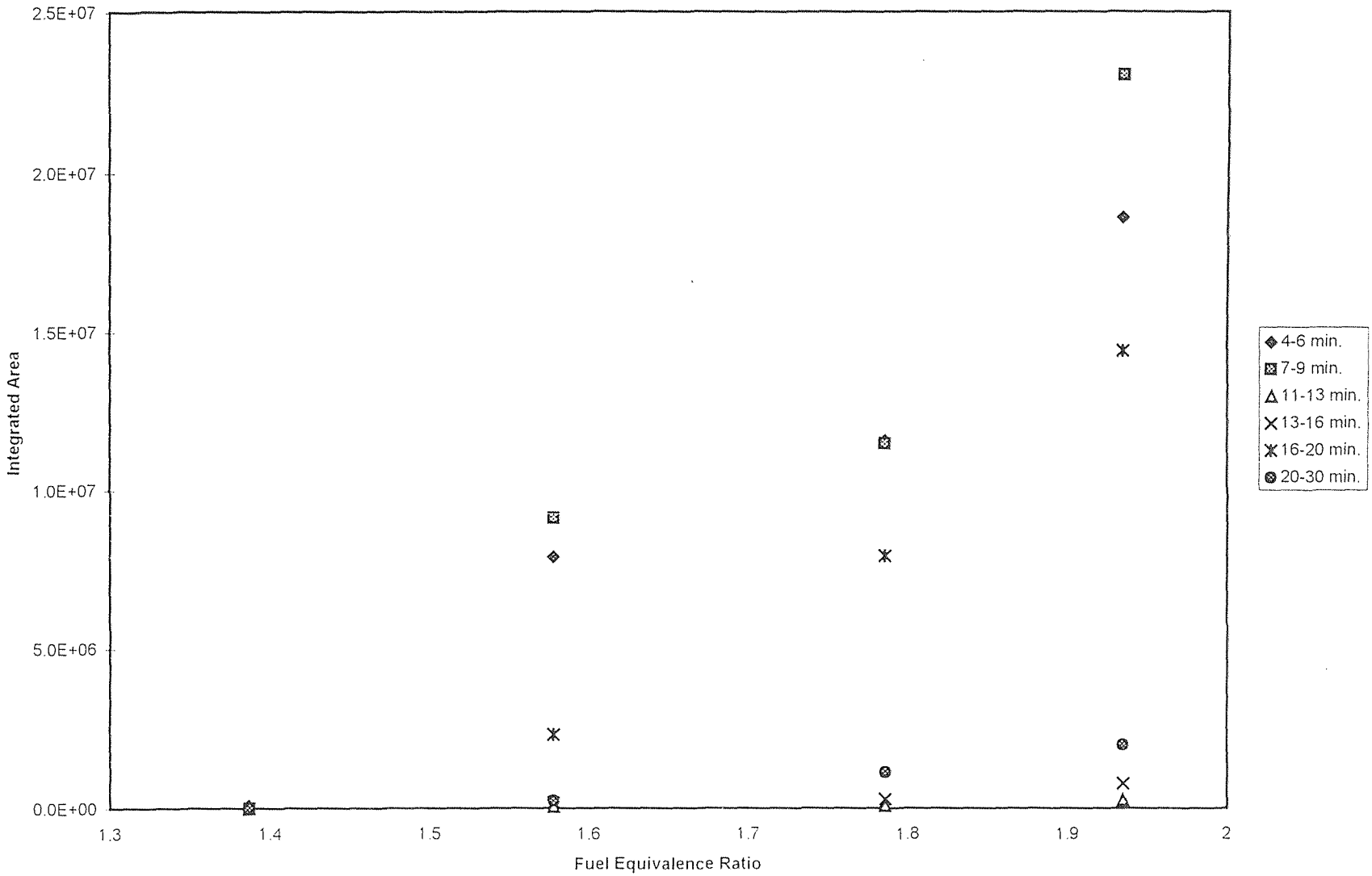

Figure 6.8 - Integrated Area of Selected Retention Time Periods

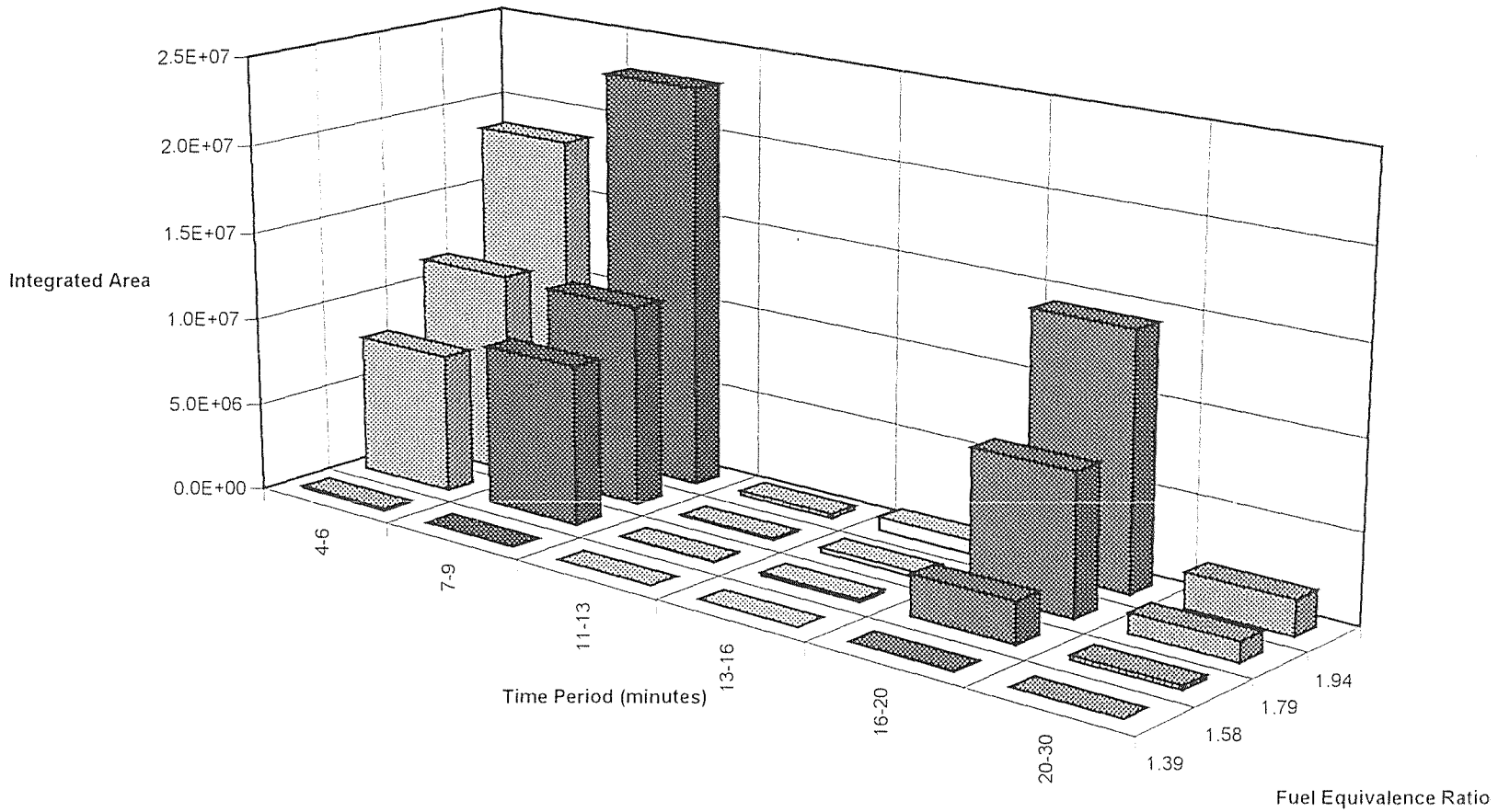

Figure 6.9 - Integrated Areas of Selected Retention Time Periods

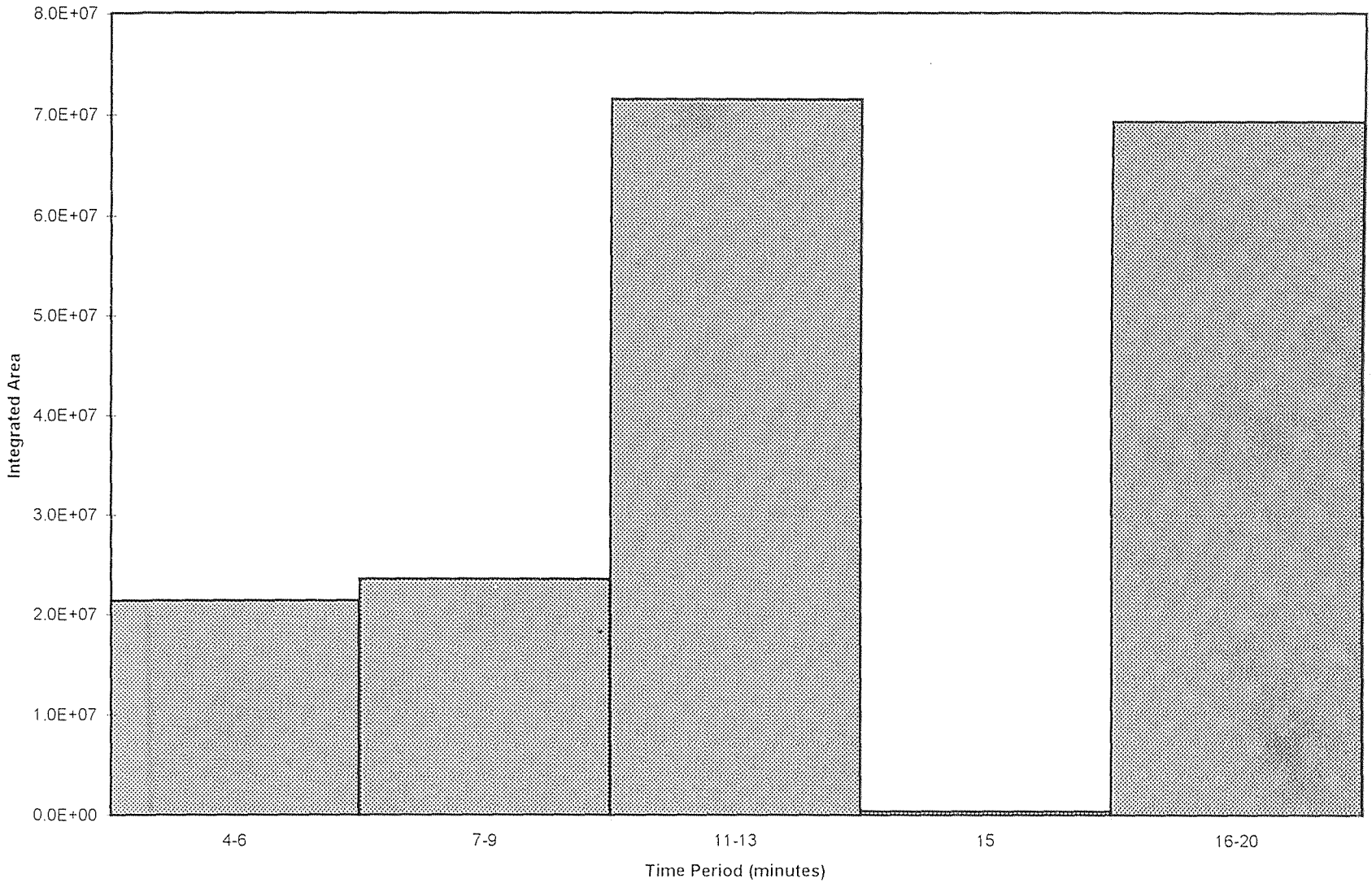

Figure 6.10 - Standard Integrated Areas of Selected Retention Time Periods

APPENDIX B

REACTOR OPERATION

Operation of Two Stage Combustor

(1) Switch on the heater in the ethylene water bath and set the temperature at 90°C. Combustor may be ignited once the bath temperature reaches 40 - 45°C.

(2) Turn on the coolant flow. Set the three lines at 10 - 15 psig and adjust according during elevated temperatures.

(3) Turn on the water sprays. Set the flow at 30 - 40 psig.

(4) Turn on the afterburner air. Set at 25 psig.

(5) Check exhaust system for vacuum pressure.

(6) Open the valve within ignition line (H_2/Air).

(7) Set the main air flowmeter at 20 at 80 psig.

(8) Set the ignition air flowmeter at 14 at 60 psig.

(9) Set the ignition hydrogen flowmeter at 2 at 55 psig.

(10) Let the gases flow for 15 - 30 seconds. Ignite the combustor by pressing the IGNITOR button. Look for the first stage temperature to jump from room temperature to about 100°C. Adjust the air flows if necessary.

(11) Flow the ethylene at 80 psig into combustor. At the same time, increase the mai air until the first stage temperature reaches or exceeds 1000°C. Set the ethylene 27 and the main air at 42 (ϕ = 0.7). ***NOTE: Take your time with this step. Th slower you increase the gas flowrates, the smoother the ignition will be.***

(12) Turn off the ignition hydrogen. Keep ignition air flowing for 2 additional minut then turn the air off and close the valve within the ignition line.

(13) Run reactor at fuel-lean conditions for at least 45 minutes, then adjust the rotame settings to achieve the desired conditions. Steady-state is achieved in approximately 45 - 90 minutes.

(14) When ready to collect sample from either the PSR or the PFR, open all relevant valves within the sample line and turn on the bellows pump.If chlorine is being burned, flow deionized water and reroute the gases through the HCl scrubber.

Adjust both the sampling valve near the bellows pump and deionized water rotameter as necessary to maintain a water leg within the column.

(15) Flush the sample lines for 30 minutes before taking data.

(16) Prior to shut-down, return to fuel-lean conditions and run for 45 minutes. Let coolant, water, and main air continue to flow through the system until all temperatures drop below 50°C.

Oxygen Continuous Emission Monitor

Refer to Mao (1995) for specific information about the carbon monoxide, carbon dioxide, nitrogen oxides, and total hydrocarbons continuous emission monitors.

(1) Be sure the power is on. Allow the CEM to run for at least one day before using.

(2) Flow nitrogen (0% O_2) through the flowmeter. Set the float at 4 and let sit for a few minutes.

(3) Set % RANGE at 10. Adjust the ZERO knob as needed.

(4) Flow standard (5% O_2) through the flowmeter. Once again, set the float at 4 and let sit for a few minutes.

(5) Adjust SPAN as necessary.

(6) When ready, flow sample through the flowmeter at the same level as used for the standard gases. Allow sufficient time before taking the reading. Change the % RANGE as needed. Avoid pegging the needle as this places unnecessary stress on the internal workings of the CEM.

Hewlett-Packard and Varian Gas Chromatographs

Before beginning, check the pressure and flowrate of each gas to be used. Set each temperature profile as well. A reference table for each column has been included.

(1) Open all three sets of hydrogen and air valves on both GCs.

(2) Allow the gases to flow for 15-30 seconds. Ignite each FID.

(3) For Column A only, open the AUX GAS valve to flow the necessary make-up nitrogen gas.

(4) Flow the respective carrier gas into each column (He or N_2).

(5) Let the GCs run for at least one half hour before injecting standard and/or sample gases.

At this point, Columns B and C are ready for gases. The third column, Column A, requires additional preparation.

(6) Set the oven temperature at 200°C and start plotting on the integrator.

(7) Push the START/RESET button on the timer in order to heat the microtrap for 1 second at 25 volts.

(8) Wait a few minutes to allow the contaminants to flow through the column. Watch for peaks on the integrator.

(9) Repeat this procedure at least three times or until the trap is clean (no peaks on the integrator).

(10) Cool the oven to 10°C using liquid nitrogen.

(11) Fill the loop with desired amount of standard or sample gas and inject. Start the C temperature profile.

(12) Wait 4 minutes. Stop the injection and push the START/RESET button on the timer.

(13) At the completion of the run, repeat the cleaning procedure described above.

Column A

Gas	Pressure (psig)	Flowrate (cc/min) at room temperature
H_2	14	30
Air	40	300
N_2 (make-up gas)	15	30
He (carrier gas)	12	3

Initial Temp.	Initial Time	Ramp	Final Temp.	Final Time
10°C	4.0 min.	5°C/min.	200°C	5.0 min.

Compound (10 ppm)	Retention Time (in minutes)
benzene	19.463

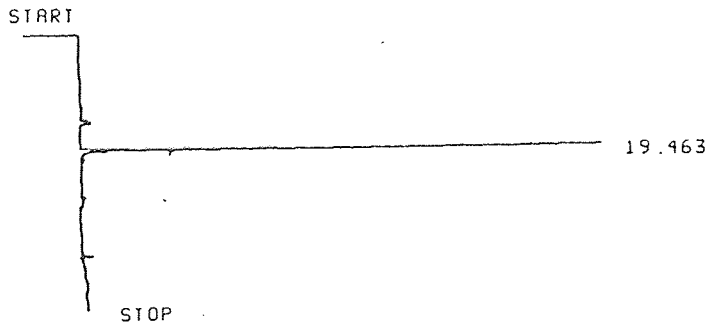

Column A
(Continued)

Compound (≈1000 ppm each)
methane
ethane
propane
butane
pentane
hexane

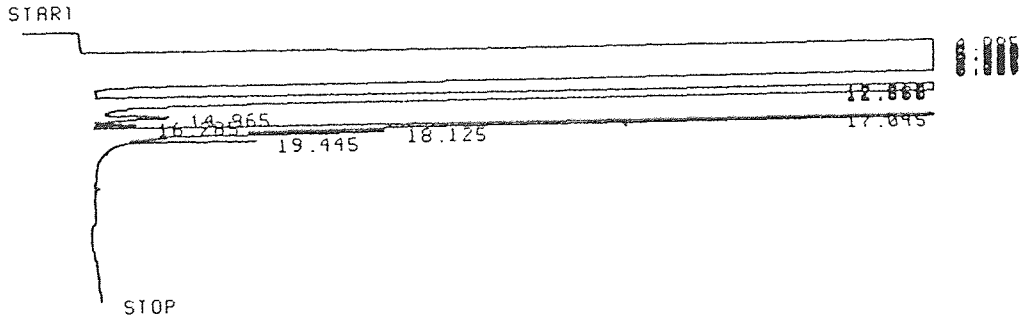

Column B

Gas	Pressure (psig)	Flowrate (cc/min) at room temperature
H_2	14	30
Air	40	300
N_2 (carrier gas)	80	30

Initial Temp.	Initial Time	Ramp	Final Temp.	Final Time
35°C	1.0 min.	5°C/min.	45°C	1.0 min.

Compound (0.1% volume of each)	Retention Time (in minutes)
methane	0.930
acetylene	1.271
ethylene	1.445
ethane	1.685

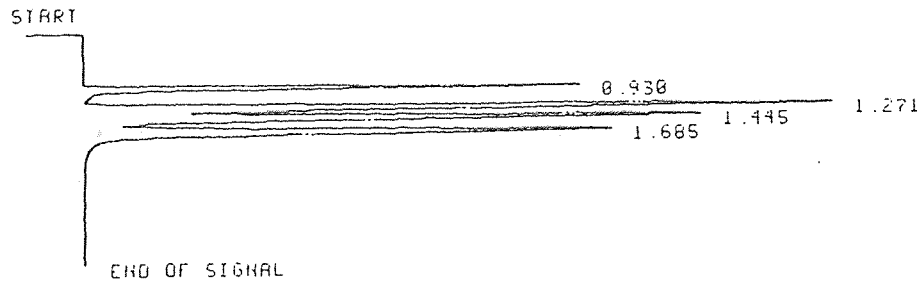

Column C

Gas	Pressure (psig)	Flowrate (cc/min) at room temperature
H_2	45	15
H_2 (catalyst converter)	10	15
Air	50	300
N_2 (carrier gas)	18	30

Initial Temp.	Initial Time	Ramp	Final Temp.	Final Time
90°C	1.7 min.	15°C/min.	110°C	20.0 min.

Compound (1.0% volume of each)	Retention Time (in minutes)
carbon monoxide	0.892
methane	1.723
carbon dioxide	3.519
acetylene	7.507
ethylene	11.125
ethane	16.446

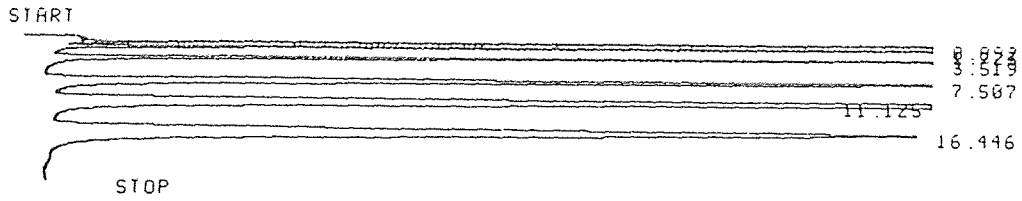

Atomizer/Vaporizer Unit

(1) If planning to use CH_2Cl_2 as the liquid, set the three thermocouple set points at the following conditions;

Heating Unit Set Point = 60°C (sufficiently above the dew point)

Heat Tracing Set Point = 50°C

Main Feed Set Point = 40°C

(2) Open the nitrogen valve on the panel and adjust the regulator until the gauge reads 30 psig.

(3) Begin flowing nitrogen through the rotameter. Set the float at 4. Let gas flow through the system for a few minutes before introducing the liquid.

(4) Once the temperatures reach their respective set points, pressurize the two glass jars by increasing the regulator until the gauge reads approximately 30 psig.

(5) Start flowing CH_2Cl_2. ***This system is very pressure sensitive. It may be necessary to adjust the pressures and flows to ensure that the liquid CH_2Cl_2 and gaseous nitrogen are flowing in the correct direction. Work slowly - CH_2Cl_2 is a dangerous substance and should be handled with caution at all time.***

(6) Watch the temperatures, pressures, and liquid levels throughout its use.

(7) When finished, reduce the pressure within the vessels via the regulator. Keep the liquid rotameter open for a few additional minutes to further allow for pressure reduction.

(8) Close the liquid rotameter, but continue flowing the nitrogen.

(9) Reduce the three thermocouple set points to room temperature.

(10) Turn off the nitrogen once the temperatures lower to room temperature.

REFERENCES

Barat, R. B., 1990, *Characterization of the Mixing/Chemistry Interaction in the Toroidal Jet-Stirred Combustor*, Ph.D. Dissertation, Massachusetts Institute of Technology, Cambridge, MA.

Barat, R. B., 1992, *Combustion Science and Technology*, Vol. 84, p. 187.

Barat, R. B., A. F. Sarofim, J. P. Longwell, and J. W. Bozzelli, 1990, *Combustion Science and Technology*, Vol. 74, p. 361.

Beer, J. M. and N. A. Chigier, 1983, *Combustion Aerodynamics*, Krieger Publishing, Malabar, FL.

Brezinsky, K., A. B. Lovell, I. Glassman, 1990, *Combustion Science and Technology*, Vol. 70, p. 33.

Brouwer, J., J. P. Longwell, A. F. Sarofim, R. B. Barat, and J. W. Bozzelli, 1992, *Combustion Science and Technology*, Vol. 85, p. 87.

Brouwer, J., G. Sacchi, J. P. Longwell, and A. F. Sarofim, 1994, *Combustion and Flame*, Vol. 99, p. 231.

Chiang, Hong-Ming, 1995, *Dichloromethane Pyrolysis and Oxidation: Formation of Chlorinated Aromatic Precursors to PCDD/F*, Ph.D. Dissertation, New Jersey Institute of Technology, Newark, NJ.

Dean, A. M., 1985, *Journal of Physical Chemistry*, Vol. 89, p. 4600.

Glarborg, P., R. J. Kee, J. F. Grcar, and J. A. Miller, 1986, *Sandia National Laboratories Report*, SAND86-8209.

Glarborg, P., J. A. Miller, and R. J. Kee, 1986, *Combustion and Flame*, Vol. 65, p. 177.

Hindmarsh, A. C., 1982, *10^{th} IMACS World Congress on System Simulation and Scientific Computation*, Vol. 1, p. 427.

Ho, W., 1993, *Pyrolysis and Oxidation of Chloromethanes, Experiments and Modeling*, Ph.D. Dissertation, New Jersey Institute of Technology, Newark, NJ.

Ho, W., R. B. Barat, and J. W. Bozzelli, 1992, *Combustion and Flame*, Vol. 88, p. 265.

REFERENCES
(Continued)

Hottel, H. C., G. C. Williams, and G. A. Miles, 1967, *11th Symposium (International) on Combustion*, The Combustion Institute, p. 771.

Kee, R. J. and J. A. Miller, 1986, *Sandia National Laboratories Report*, SAND86-8841.

Lam, F. W., 1988, *The Formation of Polycyclic Aromatic Hydrocarbons and Soot in a Jet-Stirred/Plug-Flow Reactor*, Ph.D. Dissertation, Massachusetts Institute of Technology, Cambridge, MA.

Lam, F. W., J. P. Longwell, and J. B. Howard, 1990, *23rd Symposium (International) on Combustion*, The Combustion Institute, p. 1477.

Longwell, J. P. and E. Bar-Ziv, 1989, *Combustion and Flame*, Vol. 78, p. 99.

Lovell, A. B., K. Brezinsky, I. Glassman, 1990, *23rd Symposium (International) on Combustion*, The Combustion Institute, p. 1063.

Mao, F., 1995, *Combustion of Methyl Chloride, Monomethyl Amine, and their Mixtures in a Two Stage Turbulent Flow Reactor*, Ph.D. Dissertation, New Jersey Institute of Technology, Newark, NJ.

Mao, F. and R. B. Barat, 1996, *Chemical Engineering Communications*, Vol. 145, p. 1.

Miller, J. A. and C. T. Bowman, 1989, *Progress in Energy and Combustion Science*, Vol. 15, p. 287.

Mitra, S., July 1996, Personal Communication.

Mitra, S. and A. Lai, 1995, *Journal of Chromatographic Science*, Vol. 33, p. 285.

Nenninger, J. E., 1983, *Polycyclic Aromatic Hydrocarbon Production in a Jet-Stirred Combustor*, Ph.D. Dissertation, Massachusetts Institute of Technology, Cambridge, MA.

Sarofim, A. F. and J. P. Longwell, 1996, Poster presented at the *SAC Meeting*, Newark, NJ.

Smedley, J. M., A. Williams, and K. D. Bartle, 1992, *Combustion and Flame*, Vol. 91, p. 71.

REFERENCES
(Continued)

Tonouchi, J. H., D. T. Pratt, and R. C. Steele, 1994, Poster presented at the *25th Symposium (International) on Combustion*, The Combustion Institute.

Vaughn, C. B., W. H. Sun, H. B. Howard, and J. P. Longwell, 1991, *Combustion and Flame*, Vol. 84, p. 34.

Wendt, J. O. L., 1994, *25th Symposium (International) on Combustion*, The Combustion Institute, p. 277.

Zhong, X. and J. W. Bozzelli, 1996, *International Journal of Chemical Kinetics*, In Review.